BMC Veterinary Research

RESEARCH

Open Access

Efficacy of zinc oxide and copper oxide nanoparticles on virulence genes of avian pathogenic *E. coli* (APEC) in broilers

Fawzia A. El-Shenawy[1], Eman M. El. El-Sherbeny[2] and Samr Kassem[3*]

Abstract

Background Colibacillosis is one of the broilers' most dominant bacterial diseases, either as a primary or a secondary infection. As *E. coli* antimicrobial drug resistance is rising; there is a need to develop new approaches to its control. In light of this, a comparative study of the *in-vitro* antibacterial activity of Arabic gum stabilized zinc and copper nanoparticles (AG-ZnNPs and AG-CuNPs) against PCR-identified field avian pathogenic *E. coli* (APEC) strains and virulence genes (*ibeA, hlyA, iss, pap C* and *ompA*) was applied to study the therapeutic effect of zinc and copper nanoparticles to be used as an antibiotic alternative (Nanobiotic). Furthermore, the *in-vivo* effects of CuNPs were evaluated. Additionally, the CuNPs liver and muscle residues with or without infection were examined. The eighty broilers were divided into four groups; G1: negative control, G2: infected control with *E. coli* O17, G3: non-infected treated (AG-CuNPs 50 mg/kg body weight), and G4: infected treated (AG-CuNPs 50 mg/kg body weight). AG-CuNPs treatment was given to broilers for five days in drinking water.

Results *E. coli* was isolated from diseased broilers at an average incidence rate of 20% from intestinal and liver samples. All identified serotypes (O17, O78, O91, O121, and O159) were resistant to AG-ZnNPs and sensitive to AG-CuNPs. AG-CuNPs minimal inhibitory and bactericidal concentrations (MIC and MBC) for O17 were 7.5 and 60 mg/ml, respectively. Conventional uniplex PCR results showed that strain O17 contained virulence genes (*ibeA, hlyA, iss*, and *papC*), where AG-CuNPs significantly reduced the expression of all target genes when examined by Real-time quantitative PCR. Additionally, the bactericidal activity of AG-CuNPs on O17 was 100% at 20 minutes and 40 mg/ml and confirmed by transmission electron microscopy. Furthermore, no mortality was recorded in treated groups compared to G2. Subsequently, no *E. coli was* re-isolated from the liver in the G4 after treatment. The total protein, albumin, globulin, and lysozyme activity were significantly increased in G4 compared to G2, while the activities of liver enzymes (alanine aminotransferase (ALT), Gamma-glutamyl transferase (GGT), and alkaline phosphatase (ALP)) were markedly decreased in G4 compared to G2. Additionally, uric acid, creatinine, and C-reactive protein levels were decreased in G4 compared to G2. However, the liver enzymes, kidney functions, C-reactive protein levels, and Cu residues were non-significantly changed in G4 compared to G1.

Conclusion Green synthesized AG-CuNPs are recommended as an effective antimicrobial alternative against APEC strains.

*Correspondence:
Samr Kassem
vet_doctor_2007@yahoo.com

Full list of author information is available at the end of the article

Keywords Arabic gum, Zinc oxide nanoparticles, Copper oxide nanoparticles, Avian pathogenic *E. coli*, Virulence genes, Antimicrobial alternatives, Cu residues

Background

Colibacillosis is the most dominant bacterial disease in broilers. It is considered as one of the most important multi-systemic diseases. It causes various symptoms at all ages, either as a primary or secondary infection. *E. coli* that cause disease within the avian host is categorized as avian pathogenic *E. coli* (APEC). It induces localized and systemic infections, leading to poultry production loss and quick mortality [1]. Furthermore, APEC can induce human diseases using *in-vitro* and *in-vivo* models, suggesting its zoonotic potential; therefore, it is considered a public health concern [2]. Although no distinct virulence feature has been established to recognize an APEC, there are some known virulence markers or mechanisms for APEC to cause colibacillosis in poultry. The Identified virulence markers of APEC include adhesions, toxins, iron acquisition mechanisms, invasions, and plasmids [3]. Various studies have revealed that these virulence markers are rarely present in the same isolate strain; however, single or multiple virulence markers can be detected in clinical isolates with different percentages [4].

By increasing the restriction of antibiotic growth promoter usage in poultry production, it can be speculated that colibacillosis would become an even more significant problem on commercial farms. Furthermore, treating bacterial *E. coli* infections is gradually complicated by the ability of bacteria to induce resistance to antimicrobial agents. Therefore, antimicrobial drug resistance of *E. coli* is considered a crucial public health problem and attracts poultry veterinarians' concern [5].Hence, several new approaches have been applied to control microbial infection, such as metal oxide nanoparticles (MONPs), a new class of materials for potential use in scientific research and health-related applications. Indeed, nanotechnology can be used in the pharmaceutical industry, animal health, veterinary medicine, and various extents for animal production. It is considered an effective, eco-friendly, and low-cost strategy for disease control.

Nanoparticles (NPs) have been demonstrated as proficient therapeutic agents due to their outstanding physicochemical properties, characteristics, and universally applicable physical mode of action [6].Thus, they are considered safe and effective biocidal compounds to counteract poultry bacterial infections [7]. Recently, metal nanomaterials have been used as an antimicrobial against communal infectious agents without inducing antibiotic resistance in the organisms [8].

Diverse simultaneous mechanisms of action of NPs against bacteria would make it hard for the microbes to develop resistance; thus, multiple simultaneous gene mutations inside the bacterial cell should be required to develop this resistance [9]. Additionally, some inorganic NPs are non-toxic because they contain minerals essential to the body. Most metallic NPs and metal oxide NPs have antibacterial activity, such as silver, titanium, copper oxide, and zinc oxide. Most of the antimicrobial action of NPs occurs due to their penetration and diffusion through the cell membrane of organisms, leading to the generation of oxidative stress, which destroys the microbial cells [10].

Indeed, MONPs were manufactured on a large scale and grew exponentially worldwide; therefore, they are extensively used in various fields of biomedical applications due to their increased bioavailability and endothelial cell adsorption, simple preparation processes, easy engineering to the desired size, shape, and porosity, and easy incorporation into hydrophobic and hydrophilic systems. In addition, they are less toxic than salts of the same metals, with a prolonged effect on biological objects and many novel properties compared with bulk materials [11]. Thus, easy, cheap, and eco-friendly approaches paid more attention to formulating metallic NPs to avoid the hazards of the chemical synthesis of NPs and their byproducts [12]. In light of this, Arabic gum was used in this study as a green route approach for NPs formulation. Furthermore, CuNPs gained extensive research interest due to their immense biological benefits. They exhibited beneficial effects on immunological parameters and had high bioavailability, improved growth performance, and decreased pathogenic load to enhance broilers' health [13]. In addition, their antimicrobial activity against various gram-positive or negative bacteria was reported [14]. Moreover, ZnNPs enter the intestinal cells through direct penetration and grant more beneficial effects at low doses for both livestock and the environment, besides being highly bioavailable, exerting a superior efficacy, and being more bioactive than zinc in bulk formulation [15].They have many applications as antimicrobial abilities against some pathogens.

Different biological responses to NPs occur inside the *in-vivo* systems. Therefore, more *in-vivo* studies are needed to examine the main relationship between the used *in-vitro* dose, physicochemical features of NPs, and their mode of action in disease pathophysiology to achieve the safest effective dose for treatment, optimize therapeutic benefits, and safeguard their commercial application in the poultry industry. Furthermore, these items will be beneficial to overcome biological barriers, for instance, improving the targeting and reducing the

accumulation in non-targeted cells, tissue, and organs [13].

However, several studies showed the beneficial and hazardous effects of Cu or Zn NPs as nutritional supplements, few studies reported the therapeutic effect against poultry pathogens as an antibiotic alternative (Nanobiotic). In this concern, this study aimed to explore the *in-vitro* antibacterial activities of AG-Cu and Zn NPs against various field-isolated APEC strains. Additionally, sensitivity tests, such as minimal inhibitory and bactericidal concentrations (MIC and MBC), were performed to investigate their efficacy besides using antibiotics for judging susceptibility patterns. Moreover, the strain with the highest number of virulence genes (*E. coli* O17) was used to examine the efficacy of the used CuNPs on these genes using real-time quantitative PCR (RTQ-PCR), besides estimating the effect of concentration and time on its antibacterial performance.

Furthermore, a transmission electron microscope (TEM) was used to confirm AG-CuNPs bactericidal mechanism. Subsequently, AG-CuNPs were the most effective ones. They were used *in-vivo* on broiler chickens to develop a method for predicting the therapeutic effectiveness of green synthesized nanoscale preparations as an eco-friendly approach for the biogenic production of Arabic gum-stabilized CuNPs. Moreover, their effects on clinical signs, *E. coli* re-isolation and count, non-specific immunity (lysozyme activity, total proteins, and globulin), anti-inflammatory C-reactive protein, liver enzymes activities (alanine aminotransferase (ALT), gamma-glutamyl transferase (GGT), and alkaline phosphatase (ALP)), uric acid, and creatinine levels were studied in non-infected and infected broilers. Additionally, Cu residues in both muscles and liver with/without infection were evaluated using atomic absorption spectrophotometer to avoid consumer residue problems.

Materials and methods

Collection of samples

Samples from the liver and intestine were obtained from diseased broiler chickens; all samples were collected under aseptic conditions and transferred to the bacteriological lab.

Isolation and identification of E. coli from collected samples

All collected samples were cultured on nutrient broth and incubated at 37 °C/24 h for enrichment. Then, a loop full of nutrient broth was cultivated on eosin methylene blue (EMB) agar media and incubated aerobically for 24 h. Next, pure suspected colonies were examined microscopically by gram staining and tested biochemically for identification and confirmation [16]. Finally, isolated pure colonies were sub cultured on sheep blood agar plates and incubated for 24 h aerobically to detect the suspected pathogenic strain [17].

Serological typing and identification of E. coli isolates

Obtained *E. coli* isolates were serologically identified [18] using rapid diagnostic *E. coli* antisera sets (DENKA SEIKEN Co., Japan) to diagnose Enteropathogenic types.

Molecular detection of virulence genes in isolated APEC strains using conventional uniplex PCR (cPCR)

Procedures were performed according to the instruction of the Laboratory for Poultry Production of Zagazig lab, Animal Health Research Institute, Egypt [19]. Five serotypes of isolated samples were selected to detect the virulence genes (*ibeA, hlyA, iss, papC, and ompA*). First, the extraction of DNA was performed according to QIAamp DNA mini kit instructions. Then, PCR Master Mix was prepared according to EmeraldAmp GT PCR master mix (Takara) Code No. RR310A kit as follows, 12.5 µl of EmeraldAmp GT PCR master mix (2x premix), 4.5 µl of PCR grade water, 1 µl of forward primer (20 pmol),1 µl of reverse primer (20 pmol), and 6 µl of template DNA. Subsequently, 25 µl of this mixture was used for agarose gel electrophoresis [20]. Oligonucleotide primer sequences used in cPCR are shown in Table 1.

Preparation of experimental infective dose of APEC O17strain culture for challenge assay

E. coli O17 serotype strain was previously isolated from liver samples and *enclosed* four virulence genes when subjected to molecular PCR. The pure *E. coli* O17 isolate was cultured on EMB and incubated aerobically at 37 °C/24 h. Colonies were picked up and inoculated on saline to obtain the stock inoculum for infection. The infective dose was enumerated to achieve 1×10^8 CFU/ml, and chickens were inoculated orally at two weeks old [25].

Preparation of metal nanoparticles

Arabic gum (Hashab) from the Acacia tree in Sudan was purchased from a local market. Zinc sulfate heptahydrate ($ZnSO_4.7H_2O$), sodium hydroxide (Na OH), copper (II) sulfate pentahydrate ($CuSO_4{\cdot}5H_2O$), and L-ascorbic acid were purchased from Sigma Aldrich, USA. All the chemicals were of analytical grade and used without further purification. All the synthesis was carried out using deionized water.

Synthesis of arabic gum stabilized ZnNPs (AG-Zn NPs)

The ZnNPs were prepared by a green method using $ZnSO_4.7H_2O$ and Na OH as precursors at a molar ratio of 1:2 and AG as stabilizing agent, according to Geetha et al. [26] with a modification. First, a concentration of 1.5% AG (0.043 g) was prepared in 100 ml of deionized

Table 1 Primers sequences, target genes, amplicon sizes and cycling conditions for conventional PCR and real time quantitative-PCR

Target gene	Primers sequences	Reverse transcription	Primary denaturation	Amplification (40 cycles)			Reference
				Secondary denaturation	Annealing (Optics on)	Extension	
ibeA	TGGAACCCGCTCGTAATATAC CTGCCTGTTCAAGCATTGCA	65˚C/ 60 min.	95˚C/ 15 min.	95˚C/ 15 s.	60˚C/ 1 min.	72˚C/ 30 s.	[19]
hlyA	AACAAGGATAAGCACTGTTCTGGC ACCATATAAGCGGTCATTCCCGTCA						[21]
Iss	ATCACATAGGATTCTGCCG CAGCGGAGTATAGATGCCA						[22]
papC	GTGGCAGTATGAGTAATGACCGTTA ATATCCTTTCTGAGGGATGCAATA						[23]
ompA	GGTGTTGCCAGTAACCGG GGTGGTGCACTGGAG TGG						[19]
16 S rRNA	GACCTCGGTTTAGTTCACAGA CACACGCTGACGCTGACCA						[24]

water. Then 2.88 g of $ZnSO_4.7H_2O$ was added to get a 0.1 M solution. The contents were kept under constant stirring using a magnetic stirrer to dissolve the zinc sulfate completely. Next, Na OH (0.2 M, 0.8 g) was prepared in 100 ml deionized water by adding dropwise and stirring for 2 h, and pH was adjusted to 10. The solution was incubated overnight and then centrifuged at 10,000 rpm at 4 °C/30 mins. The supernatant was discarded. Thus, nanoparticles were washed three times with deionized water to remove the impurities. Finally, the nanoparticles were dried at 80 °C overnight in a hot air oven for the complete conversion of zinc hydroxide into ZnNPs. A clear white color powder obtained was stored at room temperature for further use.

Synthesis of arabic gum stabilized CuNPs (AG-CuNPs)

The CuNPs were prepared using $CuSO_4{\cdot}5H_2O$ as a precursor and L-ascorbic acid as a reducing agent at a molar ratio of 1:2 according to Chawla et al. [27] with a modification. An aqueous solution of L-ascorbic acid (0.2 M, 3.52 g, 100 mL) was dropwise added to a hot aqueous solution of $CuSO_4{\cdot}5H_2O$ (80 °C, 0.1 M, 2.49 g, 100 mL) with AG (1.0%, 0.025 g) as capping and stabilized agent under continuous and gentle stirring using a magnetic stirrer for 2 h, pH is adjusted to 10 using Na OH (1 M). The mixture was centrifuged at 10,000 rpm at 4 °C/30 min, and pellets were collected and dried overnight in a hot air oven at 60 °C to form CuNPs. A brick red color powder obtained was stored at room temperature for further use.

Characterization methods

The chemical composition and interaction between functional groups were detected using Fourier transform infrared spectroscopy (FT-IR), Perkin Elmer, the UK, at the scanning range of 4000−400 cm^{-1}. Phase identification and crystalline structure of nano powders were analyzed by using X-ray Diffractometer, XRD (SHIMADZU, XRD-6000), with Cu Ka radiation. The particle size and surface charge of synthesized NPs were characterized using a NANOTRAC-WAVE II Zetasizer (MICROTRAC, USA). After that, the morphological investigation of synthesized NPs was detected by transmission electron microscopy (TEM) (JEM-2100, JEOL).

Cytotoxicity assay

Oral epithelial cells (OEC) were incubated in DMEM media supplemented with streptomycin, penicillin, and 10% fetal bovine serum in a 5% (v/v) humidified CO_2 atmosphere at 37 °C. Cell viability was assessed by the sulforhodamine B (SRB) assay [28]. Briefly, aliquots of 100 µL cell suspension (5×10^3 cells) were added to 96-well plates and incubated for 24 h with complete media. Next, cells were treated with another aliquot of 100 µL media containing AG-Cu and Zn NPs at various concentrations (0.31, 0.62, 1.25, 2.5, 5, 10, 20, 30, 40, and 50 mg/ml). After 72 h, cells were fixed by replacing media with 150 µL of 10% trichloroacetic acid (TCA) and incubated at 4 °C for 1 h. After washing, aliquots of 70 µL SRB solution (0.4% w/v) were added and incubated at room temperature in a dark place for 10 min, followed by washing with 1% acetic acid three times and drying in air. Then, 150 µL of TRIS (10 mM) was used to dissolve SRB stain protein bounds. The absorbance was measured at 540 nm using a BMGLABTECH®- FLUOstar Omega microplate reader (Ortenberg, Germany).

In-vitro Antibacterial activity tests

Inoculum standardization for sensitivity tests

The bacterial inoculums were adjusted photometrically using a spectrophotometer at 625 nm to give absorbance from (0.08–0.1) to approximately (1.5×10^8) CFU/ml equal to 0.5 McFarland's standard [29] to be used in agar sensitivity and MIC assays.

Antimicrobial susceptibility test (AST) assay

The antibacterial activity of both AG-Zn and Cu NPs against inoculated agar with the identified *E. coli* strains, including O17, O78, O91, O121, and O159, was assessed using the agar well diffusion method [30]. A sterile cork borer of 6 mm in diameter was used to make the wells. Subsequently, about 100 µL of Zn and Cu NPs (at concentrations of 20, 40, 60, 80, and 100 mg/ml) were filled into respective wells. After incubation at 37 °C for 24 h, the inhibition zone diameters (IZD) were measured in millimeters (mm). In addition, AST of various antibiotics, including amoxiclav AMC (30 µg), cefotaxime CTX (30 µg), gentamicin GEN (10 µg), doxycycline (30 µg), sulphamethoxazole-trimethoprim (Cotrimoxazole) COT (25 µg) and enrofloxacin ENR (5 µg) from six different families of commercial antibiotics β-lactamases-inhibitors, cephalosporins, aminoglycosides, tetracyclines, folates-inhibitors, and quinolones was performed using disk diffusion method to judge the susceptibility patterns and IZD of the used drugs. Results were classified as susceptible, intermediate, or resistant by measuring IZD [31]. Each antimicrobial assay was performed simultaneously in triplicate.

MIC and MBC values

The MIC as a quantitative bioassay was determined by using a micro-broth dilution test in a 96-well microplate using standard guidelines of CLSI [31] against the identified *E. coli* strains; O17, O78, O91, O121, and O159. A 60 mg/ml solution of CuNPs was twofold serially diluted to 0.127 µg/ml. Both negative (only drug without bacteria) and positive (only bacteria without drug) control wells were prepared. Referring to the results of the MIC assay, a loopful from each clear well was streaked on the EMB agar, incubated at 37 °C/24 h, and then observed for growth. The lowest concentration that showed no turbidity was recorded as the MIC, and the lowest concentration that did not show any growth was recorded as the minimum bactericidal concentration (MBC). The experiment was performed in duplicate. In addition, TEM was used to study the antibacterial effect of AG-CuNPs on *E. coli* O17 cultures after incubation with 50 mg/ml of CuNPs at 37 °C/overnight, then processed and observed in JEOL 1400 (JEOL, Ltd., Japan) running at 80 kV [32].

Antibacterial performance of AG-CuNPs against E. coli O17 strain

The effect of time and concentration of AG-CuNPs on its antibacterial performance against *E. coli* O17 were assessed as mentioned Li et al. [33]. *E. coli* O17 was prepared in approximately 1×10^8 CFU/ml, and then 50 µl of this bacterial suspension was inoculated into 950 µl of various concentrations of AG-CuNPs. After several sterilization times, these grown bacterial suspensions were inoculated on EMB Petri dishes. This study used various times of (*E. coli* O17- AG-CuNPs) contact at intervals from 5 to 30 min with various concentrations of AG-CuNPs ranging from 5 to 60 mg/ml). Finally, all plates were incubated at 37 °C/24 h, and the number of surviving cells was counted. The number of surviving cells was calculated as a percentage compared to the positive control plates without AG-CuNPs; then, results were subtracted from 100% to obtain the antibacterial rate. Each experiment was performed in duplicate and mean values were calculated.

Detection of the efficacy of CuNPs on virulence genes expression of E. coli O17 strain by real-time quantitative PCR (qRT–PCR):

Pure *E. coli* O17 strain at a dose of 10^8 CFU/ml (the experimental challenge dose) was mixed with CuNPs at a dose of 50 mg/ml broth and incubated at 37 °C overnight, then subjected to qRT–PCR using comparative cycle threshold (CT) to detect the fold change value of the different target virulence genes expression. The treated *E. coli* strain sample containing (*ibeA, hlyA, iss, and papC*) was compared with the control non-treated *E. coli* strain sample. In addition, the relative expression of the target genes was determined in comparison to a standard reference gene of 16 S- rRNA. RNA extraction from samples (treated *E. coli* strain isolate and control non-treated *E. coli* strain isolate) was performed using QIAamp RNA mini kit instructions when 200 µl of the sample were added to 600 µl RLT buffer containing 10 µl β-mercaptoethanol per 1 ml, incubated at room temperature for 10 min. One volume of 70% ethanol was added to the cleared lysate, and these steps was completed according to the Purification of total RNA protocol of the QIAampRNeasy Mini kit (Qiagen, Germany, GmbH). Primers were utilized in a 25- µl reaction containing 10 µl of the 2x HERA SYBR® Green RT-qPCR Master Mix (Willowfort, UK), 1 µl of RT Enzyme Mix (20X), 0.5 µl of each primer of 20 pmol concentration, 5 µl of water, and 3 µl of RNA template. Amplification curves and ct values were determined by the step one software Primers sequences, target genes, amplicon sizes and cycling condition were showed in the table Table 1. The CT of the treated sample was compared with that of the control non-treated sample to estimate the gene expression variation on the treated sample's RNA according to the "ΔΔCt" method by using the following ratio: ($2^{-\Delta\Delta Ct}$). Each assay was performed simultaneously in triplicate [34].

In-vivo Assessment of the Cu NPs' antimicrobial efficacy

Experimental design

A total of 90 one-day-old broiler chicks were purchased from a private farm. Then, the livers of 10 chicks were tested bacteriologically to ensure they were free from any

systemic *E. coli* infection. The remaining 80 chicks were divided into four groups (20 chicks /group); G1: negative control, G2: positive control infected orally with *E. coli* O17 (1×10^8 CFU/ml), G3: non-infected treated with (AG-CuNPs 50 mg/kg body weight) and G4: infected treated with (AG-CuNP 50 mg/kg body weight). This effective dose of AG-CuNPs (50 mg/kg body weight) was adjusted from our *in-vitro* sensitivity tests, TEM, and cytotoxicity assays. All groups had the same management and vaccination with free access to Feed and water. Two weeks old broilers were infected and then observed daily for morbidity, mortality, clinical signs, and necropsy finding. All treatments were administered following the onset of clinical symptoms on the 20th and continued for five successive days via drinking water until the 24th day. The experiment was conducted until the 35th day of age. The animal studies were approved by Research Ethics Committee for environmental and clinical studies (Protocol number: 165,429) at Animal Health Research Institute (AHRI) and were carried out under Egyptian Ethics Committee Guidelines and the NIH guidelines for the Care and Use of Laboratory Animals. All animal experiments were performed following the ARRIVE guidelines (https://arriveguidelines.org).

Sampling

Blood samples Blood samples were collected from the wing vein (5 broilers/group) in a centrifuge tube without anticoagulant to get the serum on the 25th and 35th day related to after treatment and at the end of the study respectively. Alanine aminotransferase (ALT) [35], gamma-glutamyl transferase (GGT) [36], alkaline phosphatase (ALP) activities [37], total protein (TP) [38], and albumin [39] were determined. Globulin was detected by subtracting the albumin value from TP. For immunological evaluation, serum lysozyme activity was measured by agarose gel lysis assay [40]. The C-reactive protein, one of the anti-inflammatory parameters, was determined [41]. Uric acid [42] and creatinine [43] were estimated to evaluate kidney functions. All tests were determined using commercial kits (Spectrum and EgyChem, Egypt).

Tissue samples Liver (1 g) and intestine (1 g) from all infected groups (3 broilers/group) were collected after treatment under aseptic conditions for *E. coli* re-isolation and count. First, tissues were transferred to 9 ml phosphate buffer saline (PBS) to prepare the initial suspension. Subsequently, tenfold serial dilutions were made, and then 0.1 ml of each dilution was spread on EMB agar plates and incubated aerobically at 37 °C/24 h. Then the number of survived cells was counted. For detection of Cu residues; tissue specimens from the liver (as an edible organ), breast, and thigh muscles were collected (5 broilers/group) after treatment and at the end of the study. Residues were measured using atomic absorption spectrophotometer (AA-7000 – Shimadzu) according to the method described by Okoye et al., [44]. A schematic illustration of the experimental design were showed in Supplementary Fig. 1.

Statistical analysis

One-way analysis of variance (ANOVA) was applied for statistical analysis. Duncan multiple range post-hoc analysis tests using IBM SPSS software statistical program (version 20.0) were used to compare means at the significance level of $P<0.05$. Data were expressed as mean ± SE (standard error) and $N=5$.

Results

Incidence of E. coli isolates among examined samples

After microscopically gram staining testing, biochemical identification, and confirmation of suspected pure isolates, *E. coli* was isolated with a total incidence rate of 20% (20/100) in all examined samples collected from diseased broilers, 18% (9/50) from liver samples, and 22% (11/50) from intestinal samples.

Serological typing and characterization of E. coli isolates

Results revealed that the examined samples belonged to O17: H18, O121: H7, O78, O127: H6, O91: H21, O103: H2 and O159. O78 was the most prevalent serotype with 30%, followed by O91: H21 with 20%, followed by O17: H18 with 18%. O17 was isolated and detected only in liver samples, whereas O78 and O91 were isolated from liver and intestinal samples, and O121 and O159 were isolated from intestinal samples only.

Molecular detection of the virulence genes using uniplex cPCR

In this study work we used uniplex conventional PCR to avoid false negative results during gel electrophoresis interpretation as some gene amplification may give bands at nearly closed molecular weight, so uniplex PCR is more accurate than multiplex PCR. The *hlyA* gene was expressed in all serotyped APEC isolates. In contrast, the *ompA* gene was not expressed in all serotyped APEC isolates. However, four virulence genes, *ibeA, hlyA, iss*, and *papC*, were expressed in only the O17 serotype. The results are shown in Tables 2 and Fig. 1A-D. Individual Agarose gel electrophoresis images for PCR amplification of all virulence genes were showed in supplementary Figs. 2–5.

Characterization of AG-CuNPs and ZnNPs

Particle size and zeta potential

The results of Zetasizer showed that the average particle size of Cu and Zn NPs was58nm and 75 nm, respectively,

Table 2 Molecular detection of the virulence genes using uniplex cPCR

Serotyped isolate	*ibeA*	*hlyA*	*iss*	*papC*	*ompA*
O 17	+	+	+	+	-
O 78	-	+	+	+	-
O 91	-	+	-	-	-
O 121	-	+	+	-	-
O 159	-	+	-	+	-

with a narrow size distribution; poly dispersity index (PDI) was0.16 and 0.15, respectively, and surface charges of-24.8 and −25.5 mV, respectively (Fig. 2A1 and A2).

X-ray diffraction studies

The XRD pattern of synthesized AG-Cu and ZnNPs is shown in Fig. 2B1 and B2. For the CuNPs, prominent peaks can be observed at 2θ of 43.3, 50.4, 74.1, 89.9, and 95.1°. The assignments of 2θ position and other parameters for AG-CuNPs from XRD agree with the reference code (COD-9,012,043) at a wavelength of 1.54060 with a cubic crystal system and space group Fm-3 m.For the

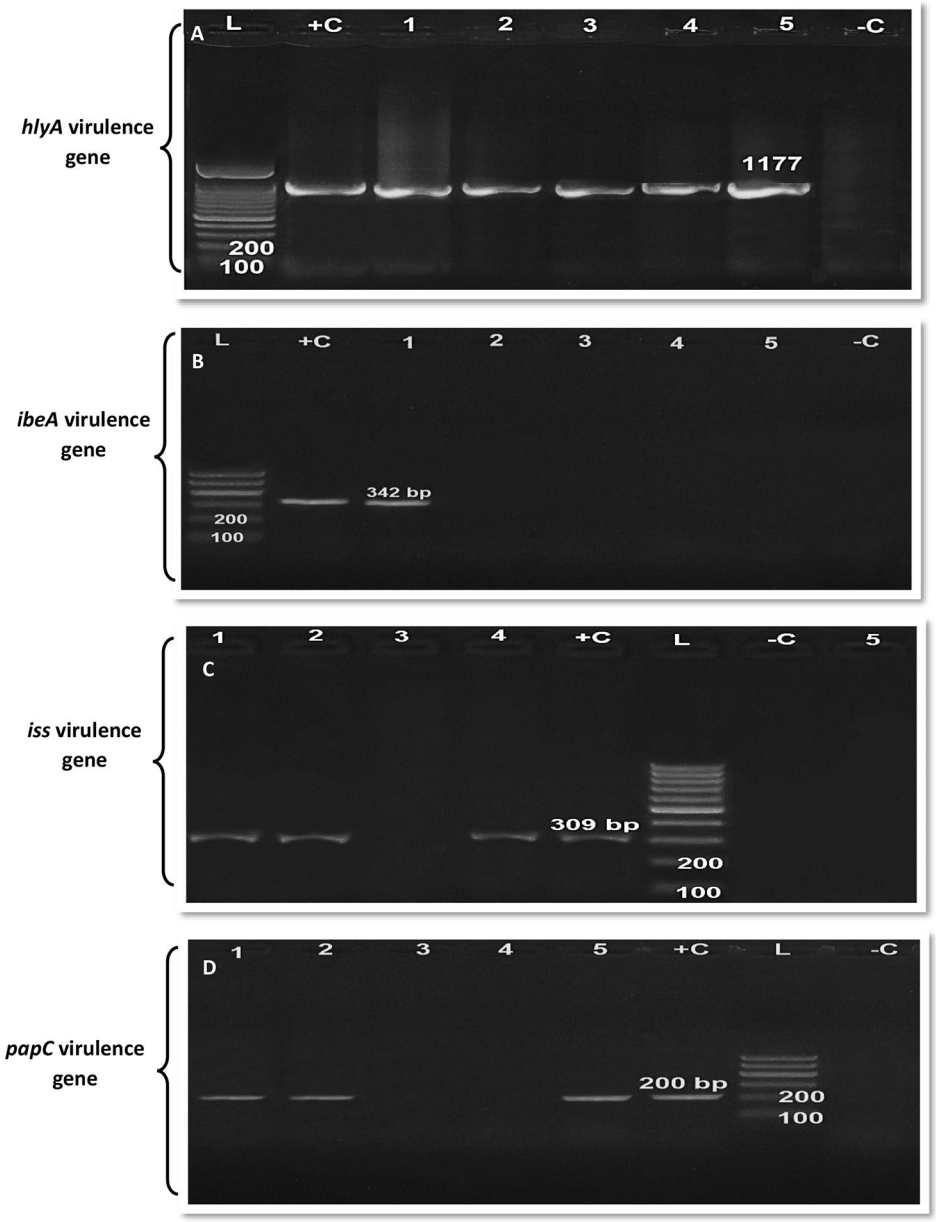

Fig. 1 Grouping of 4 separate images for (**A**) Agarose gel electrophoresis for PCR amplification of *hlyA* virulence gene at (1177 bp), (**B**) *ibeA* virulence gene at (342 bp), (**C**) *iss* virulence gene at (309 bp), (**D**) *papC* virulence gene at (200 bp) in APEC serotypes: Lane L (ladder), Lane + C (control positive), Lane - C (control negative), Lane 1 (serotype O17), Lane 2 (serotype O78), Lane 3 (serotype O91), Lane 4 serotype (O121) and Lane 5 (serotype O159)

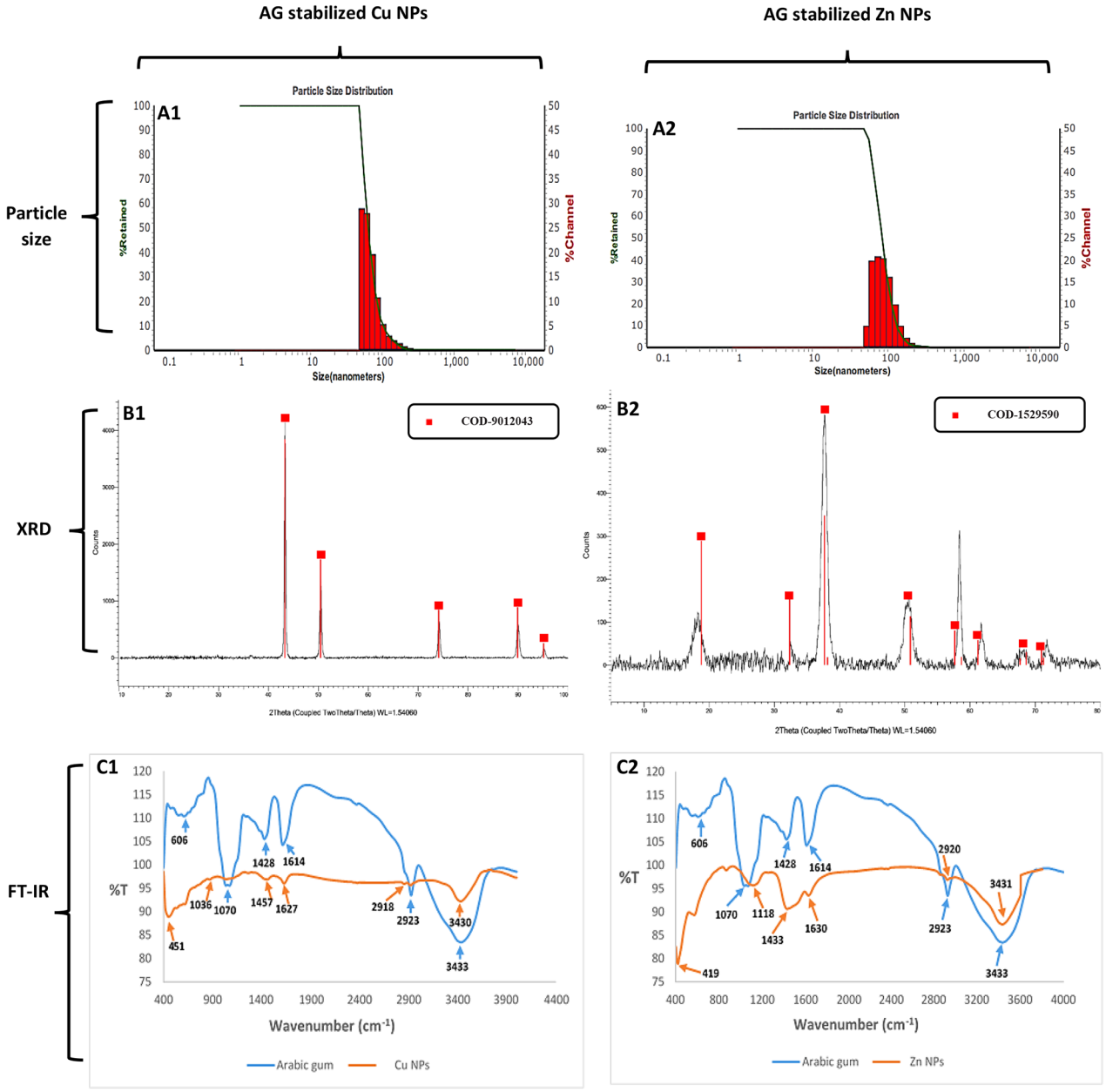

Fig. 2 Characterization of AG stabilized Cu and ZnNPs. (**A1** and **A2**) particle size pattern of synthesized NPs showing (**A1**) size distribution of CuNPs of 58 nm, (**A2**) size distribution of ZnNPs of 75 nm. (**B1** and **B2**) XRD pattern of Cu and ZnNPs respectively at the wavelength of 1.54060. (**C1** and **C2**) FT-IR spectra of Cu and ZnNPs respectively at the scanning range of 4000 – 400 cm^{-1} compared with Arabic gum

AG-Zn NPs, prominent peaks can be observed at 2θ of 18.81, 32.34, 38.15, 50.86, 57.68, 61.23,68.64, and 70.96°. The assignments of 2θ position and other parameters for ZnNPs from XRD agree with the reference code (COD-1,529,590) at a wavelength of 1.54060 with a hexagonal crystal system and space group P-3m1.

FT-IR spectra

FT-IR spectra of *Arabic gum* synthesized and stabilized AG-Cu, and ZnNPs are shown in (Fig. 2; C1 and C2). For Arabic gum, the peak at 3433 cm^{-1} showed the presence of the N-H bond in stretching mode, and the peak at 2923cm^{1} showed the presence of the O-H bond in stretching mode (carboxylic acid).The peak at 1614 cm^{-1}referred to the presence of the N-H bond, which bent in primary amine. The peak at 1428 cm^{-1}showed the presence of the C-O-H bond in the bending mode, while the peaks at 1070 $cm^{-1}$and 606 cm^{-1}showed the presence of C-O and C-l bondsin the stretching mode. For AG-CuNPs, the N-H bond in stretching mode is represented at

3430 cm^{-1}, while the peak at 2918 cm^{-1} showed the presence of O-H bond stretching mode (carboxylic acid). Furthermore, the peak at1627cm^{-1}referredto the presence of the N-H bond, which bended in primary amine, while the peak at 1457 cm^{-1}referredto the presence of the N-H bond, which bent in secondary amine. The peaks at 1036 $cm^{-1}$and 451 cm^{-1} showed the presence of the C-O and C-l bond in the stretching mode.

For AG-ZnNPs, the N-H bond in stretching mode is represented at the peak of 3431 cm^{-1}, while the peak at 2920 cm^{-1}revealedthe presence of O-H bond stretching mode (carboxylic acid).In addition, the peak at 1630 cm^{-1} referred to the presence of the N-H bond, which bent in primary amine, the peak at 1433 cm^{-1} showed the presence of the C-O-H bond in the bending mode, the peak at 1118 cm^{-1} showed the presence of C-O bond in stretching mode, and the peak at 419 cm^{-1} showed the presence of C-l bond in stretching mode.

Morphological characters and cytotoxicity assay

TEM images of stabilized AG-Cu and ZnNPs (Fig. 3; A1, 2 and B1, 2) showed distinctive single NPs with spherical shapes without aggregation. Their size ranged from 7.68 to 19.5 nm for CuNPs (Fig. 3; A1 and A2) and 23.4 to 39.6 nm for AG-ZnNPs (Fig. 3; B1 and B2).

In the SRB assay, the survival rate was decreased from 98.7to 81.25% at concentrations of 0.31and 50 mg/ml, respectively, as shown in Fig. 3C for the cells incubated with different concentrations of AG-CuNPs. However, the survival rate was decreased from 101.82 to 89.23% at concentrations of 0.31 and 50 mg/ml, respectively, for the cells incubated with different concentrations of AG-ZnNPs, as shown in Fig. 3C. NPs did not show toxicity concentrations less than 50 mg/ml, and cells kept the same morphological characteristics as control ones.

In-vitro Antibacterial activity tests

AST, MIC, and MBC of AG-CuNPs against tested E. coli isolates

AST of commercial antibiotics or AG-ZnNPs indicated the complete resistance of all *E. coli* tested strains to all tested antibiotics and all of the used AG-ZnNPs concentrations from 20 to 100 mg/ml. Whereas AST of AG-Cu NPs (Table 3) revealed a significant antibacterial activity with markedly ascending IZDs against all *E. coli* tested strains corresponding to the used concentrations from 20 to 100 mg/ml. In most of the detected strains, no significant difference was recorded between IZDs of both (20 and 40) mg/ml or (80 and 100) mg/ml; for example, the AST of the *E. coli* O17 strain used in our *in-vivo* study (Fig. 4; A-C). The *E. coli* O17 strain was reported to have the highest IZD ranging from 19.66±0.33 to 25.00±0.00 mm, corresponding to the used concentration. The IZDs of AG-CuNPs reflected effective antibacterial activity that is similar to other traditional antimicrobials. Results of MIC and MBC of CuNPs varied according to the *E. coli* tested strains. MIC values were 3.75 mg/ml for O78, 7.5 mg/ml for O17, and 15 mg/ml for O91, O121, and O159, while the bactericidal effect of AG-CuNPs (MBC) was reported at 60 mg/ml well for O17, O78, and O121 only, while other O91 and O159 required higher concentrations than 60 mg/ml.

Furthermore, the bactericidal activity of AG-CuNPs on the *E. coli* O17 strain was confirmed using TEM analysis (Fig. 5; A-F),where anchoring and accumulating NPs around bacterial cell wall were recorded besides the intracellular distribution of NPs in the bacterial cytoplasm giving ghost appearance that ended with cell damage.

Antibacterial performances of AG-Cu NPs on E. coli O17 strain

Figure 6 displays the antibacterial effect of AG-CuNPs on the viability of *E. coli* O17 post-incubation with different contact times or different AG-CuNPs concentrations to meet the bactericidal activity threshold. As shown in Fig. 6A, the antibacterial rate of AG-CuNPs against *E. coli* O17 was detected from 5 to 30 min, which increased with time. The bactericidal effect appeared at 20 min when the antibacterial rate reached 100%. The effect of AG-CuNPs concentrations on *E. coli* O17 inactivation has been illustrated In Fig. 6B. Thus, the antibacterial rate was 100% at 40 mg/ml AG-CuNPs. The surviving bacteria with AG-CuNPs were significantly less than the control groups throughout all times and concentrations.

Efficacy of AG-CuNPs on target virulence genes expression of E. coli O17 strain by real-time quantitative PCR (RTQ – PCR)

The expression of virulence genes was significantly down regulated in the treated *E. coli* compared to the control non-treated sample with the treatment dose of AG-CuNPs (50 mg/ml). The *papC* gene was mostly down regulated with 0.2698, while the *ibeA*, *iss*, and *hlyA* genes were down regulated with 0.403320, 0.5396, and 0.586 respectively, as shown in Fig. 7.

In-vivo Assessment of the AG-Cu NPs antimicrobial efficacy

Clinical signs, post-mortem findings, and mortalities

Clinical signs of *E. coli* appeared on the 4th and 5th days post-infection as anorexia, depression, ruffled feathers, and diarrhea. No signs were reported in the negative control G1. Five chicks died in the infected control G2 post-inoculation and throughout the experiment where their post-mortem lesions in most carcasses displayed severe to a mild degree of visceral congestion, enlargement, congestion of liver and spleen, mild pericarditis, and precipitated urea in the ureter. Conversely, no mortality was recorded in other negative control or treated groups. As well, general health and behavior activities showed a noticed improvement post-treatment.

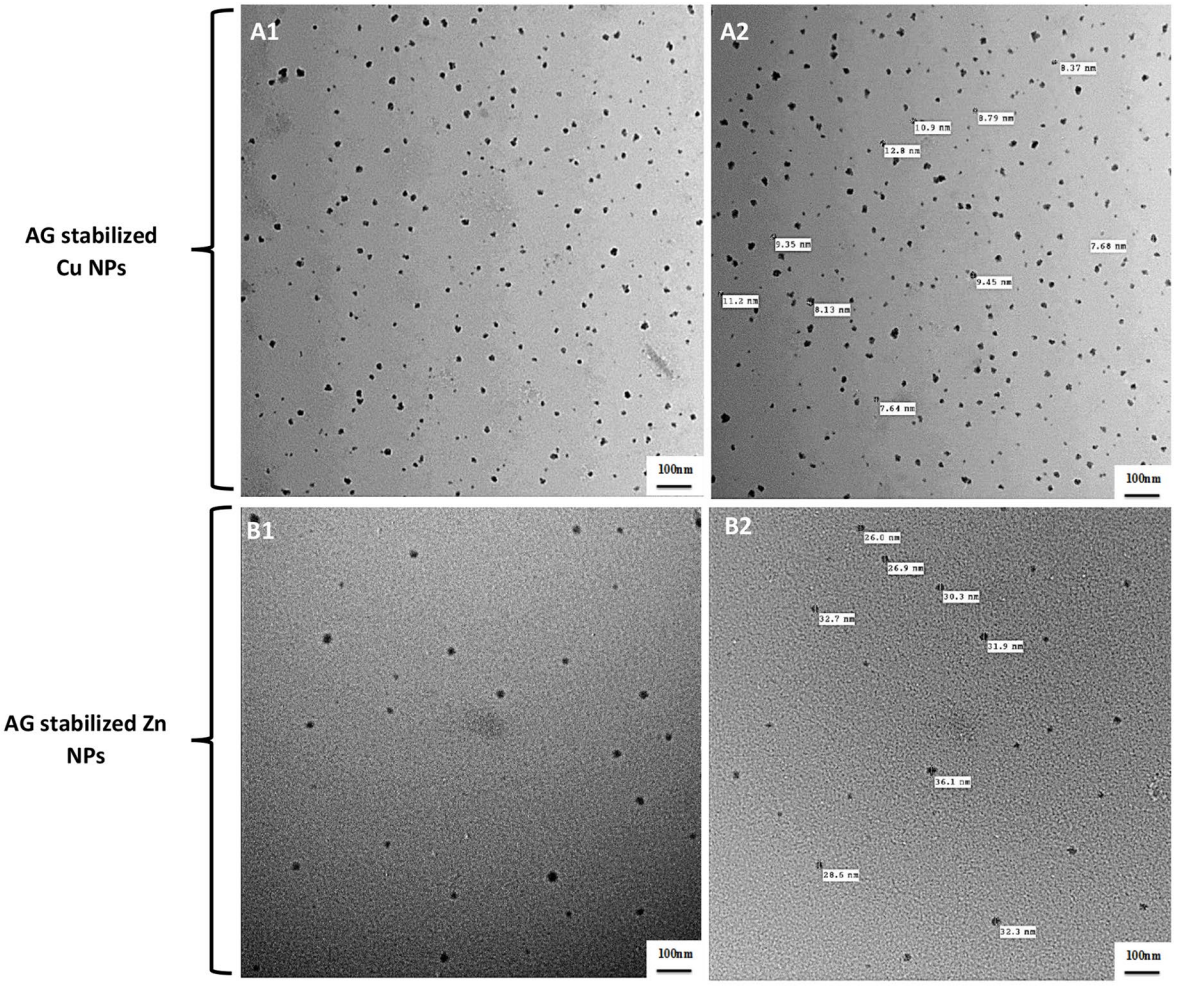

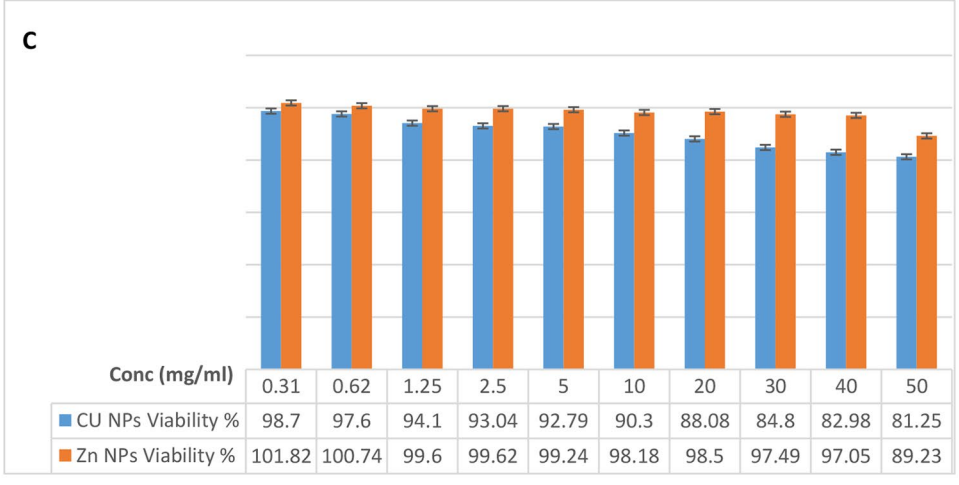

Conc (mg/ml)	0.31	0.62	1.25	2.5	5	10	20	30	40	50
CU NPs Viability %	98.7	97.6	94.1	93.04	92.79	90.3	88.08	84.8	82.98	81.25
Zn NPs Viability %	101.82	100.74	99.6	99.62	99.24	98.18	98.5	97.49	97.05	89.23

Fig. 3 Morphological characters and cytotoxicity assay of AG stabilized Cu and ZnNPs, (**A1** and **A2**) is TEM imaging of AG stabilized CuNPs showed well dispersed nanosphere particles and size ranged from 7.68 to 19.5 nm, Scale bar = 100 nm. (**B1** and **B2**) is TEM imaging of AG stabilized ZnNPs showed spherical nanoparticles without agglomeration and size ranged from 23.4 to 39.6 nm, Scale bar = 100 nm. (**C**) is SRB cytotoxicity assay of AG stabilized Cu and ZnNPs at different concentrations ranged from 0.31 to 50 mg/ml

Table 3 The inhibition zone diameters of AG-Cu NPs on isolated *E. coli* strains

Strains	Inhibition zone diameters in millimeter at various AG-Cu NPs concentrations				
	20 mg/ml	40 mg/ml	60 mg/ml	80 mg/ml	100 mg/ml
O17	19.66 ± 0.33 [a]	20.00 ± 0.00 [a]	20.00 ± 0.00 [a]	22.33 ± 0.33 [b]	25.00 ± 0.00 [c]
O78	17.00 ± 0.57 [a]	18.00 ± 0.00 [a]	20.00 ± 0.00 [b]	22.00 ± 0.57 [c]	24.00 ± 0.57 [d]
O91	16.66 ± 0.33 [a]	17.00 ± 0.00 [a]	18.33 ± 0.33 [b]	21.00 ± 0.00 [c]	22.33 ± 0.33 [d]
O121	18.00 ± 0.00 [a]	19.00 ± 0.57 [a]	21.66 ± 0.33 [b]	22.00 ± 0.00 [bc]	23.00 ± 0.57 [c]
O159	16.33 ± 0.33 [a]	18.00 ± 0.00 [b]	18.00 ± 0.57 [b]	20.33 ± 0.33 [c]	21.00 ± 0.57 [c]

The various letters in the same row indicate statistically significant differences when ($P < 0.05$) (Mean ± SE) n = 3

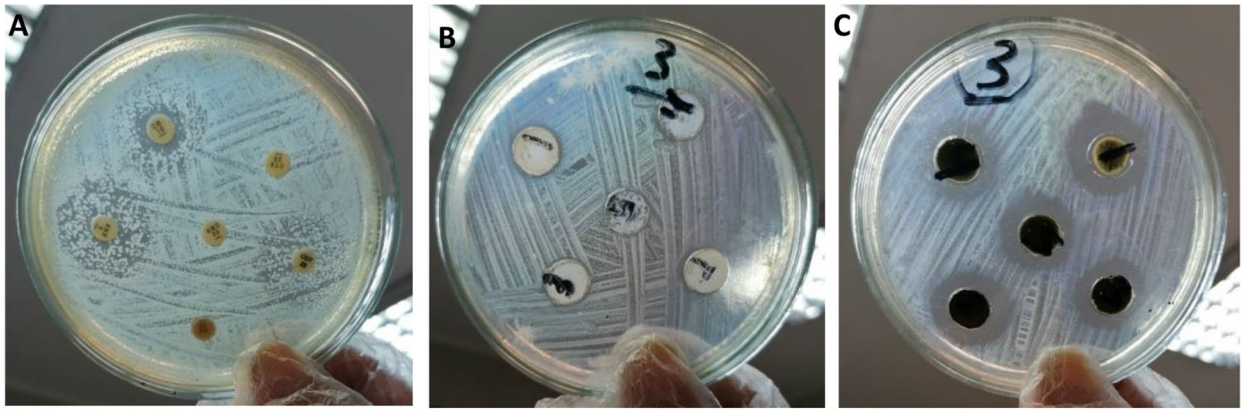

Fig. 4 Antimicrobial sensitivity tests (AST) of *E. coli* O17 strain (**A**) against commercial antibiotic disks indicated complete resistance and (**B**) against various AG-ZnNPs concentrations indicated complete resistance, while (**C**) against AG-CuNPs showed various inhibition zone diameters

E. coli re-isolation and count

No *E. coli* were re-isolated from the liver of non-infected G1 or G3, indicating the absence of systemic infection. In the infected control G2, *E. coli* counts were ($3.67 \times 10^3 \pm 0.33$) and ($50.33 \times 10^3 \pm 2.03$) CFU/g in liver and intestine samples, respectively. Post-treatment, no *E. coli* was re-isolated from liver samples of infected treated G4, while its count in intestine samples was $2 \times 10^3 \pm 0.58$ CFU/g.

Serum biochemical parameters

TP, albumin, and globulin levels were significantly decreased, while ALT, GGT, and ALP activities were significantly increased in infected control G2 compared to control G1 (Table 4). Post-treatment, TP, albumin, and globulin were non-significantly changed in non-infected treated G3 compared to G1. However, the activities of enzymes were significantly increased in non-infected treated G3 compared to G1, while at the end of the experiment, results returned to their normal levels. There were significant increases in TP, albumin, and globulin besides significant decreases in most of the detected enzymes' activities in infected treated G4 than G2. In contrast, it showed no significant difference from G1 in most of these detected parameters at the end of the experiment.

Immunological, Anti-inflammatory, and kidney function biomarkers

The lysozyme activity was significantly decreased, while C-reactive protein, uric acid, and creatinine levels were significantly increased in infected control G2 compared to control G1 (Table 5). Post-treatment and at the end of the experiment, the lysozyme activity was significantly increased, while C-reactive protein was significantly decreased with no significant effect on uric acid or creatinine in both non-infected treated G3 and infected treated G4 compared to control G1. The lysozyme activity was significantly increased, while C-reactive protein, uric acid, and creatinine levels were significantly decreased in the infected treated G4 compared to infected control G2 (Table 5).

Residues of Cu in liver and muscles

In Table 6, results of Cu residues in the liver showed a significant increase in G2 than G1. After treatment and at the end of the experiment, all treated groups G3 and G4 were significantly more than control groups G1 and G2. In muscle, Cu residues showed a significant increase in G2 than G1. After treatment, all treated groups G3 and G4 were significantly more than control groups G1 and G2, while at the end of the experiment, all treated groups revealed no significant difference from G1.

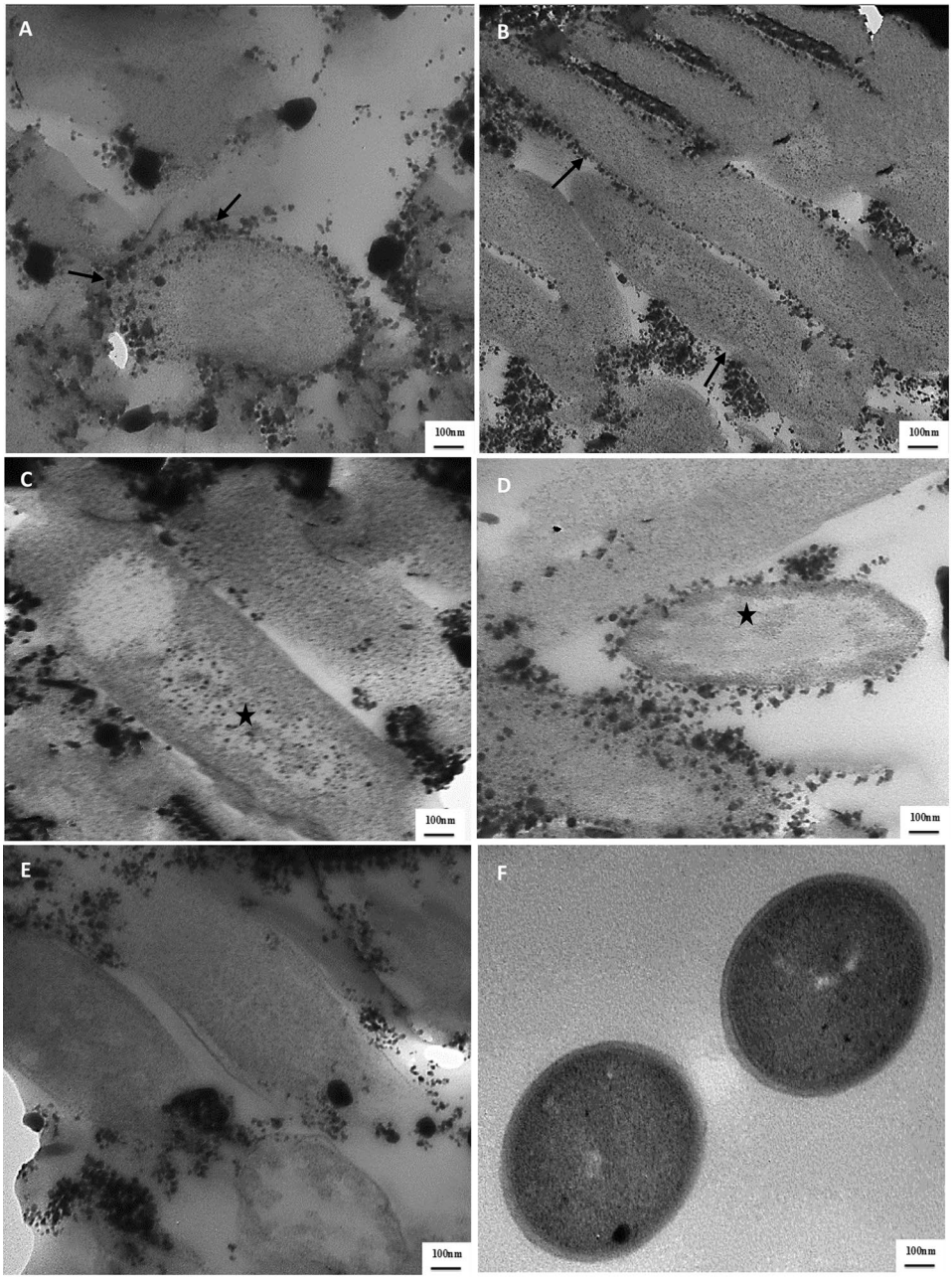

Fig. 5 TEM images of *E. coli* O17 cells grown in the media containing 50 mg/ml of AG stabilized CuNPs showed accumulation of nanoparticles on the cell wall (arrows) and attack of nanoparticles (**A**), (**B**) showed elongation of bacterial cell and particles around bacterial surface (arrows). (**C**) showed internalization of NPs intracellular and distribution in cytoplasm (star). (**D**) showed ghost appearance of cell with empty and flaccid structure (star) and cytoplasm with low electronic density. (**E**) showed disruption of cell wall and cellular damage 24 h post incubation compared with control bacterial cells only (**F**). Scale bar = 100 nm

Discussion

APEC is an infectious bacterium causing colibacillosis. Colisepticemia is the most common form of colibacillosis, which is still a significant threat to the poultry industry, causing high economic losses due to mortality and condemnations, and is a widespread disease [7]. The expansion of bacterial-resistant strains to different antimicrobials has encouraged researchers to search for other antimicrobial options. The antibacterial potentials of MONPs may introduce a probable solution to this problem. Recently, non-toxic origin-mediated synthesis of AG-CuNPs has been one of the critical roles of therapeutic bio applications. Therefore, our study was designed to compare the possible antibacterial effect of AG-Cu and Zn NPs against various field-isolated APEC strains and their virulence genes *in-vitro*. Green

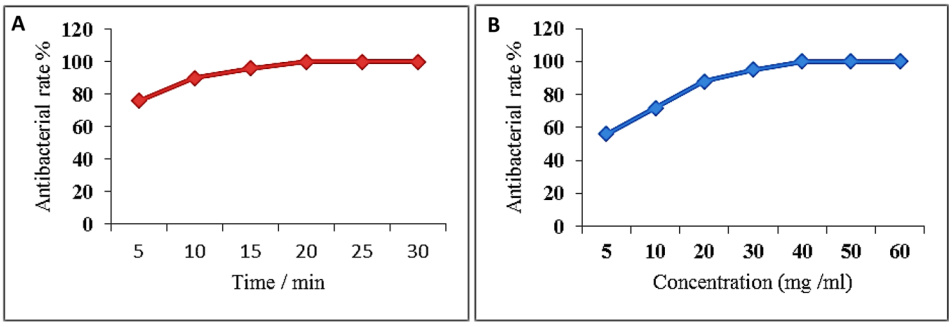

Fig. 6 (**A**) The antibacterial rates of AG-CuNPs against *E. coli* O17 isolate post various times of contact, (**B**) The antibacterial rates of AG-CuNPs against *E. coli* O17 on various concentrations

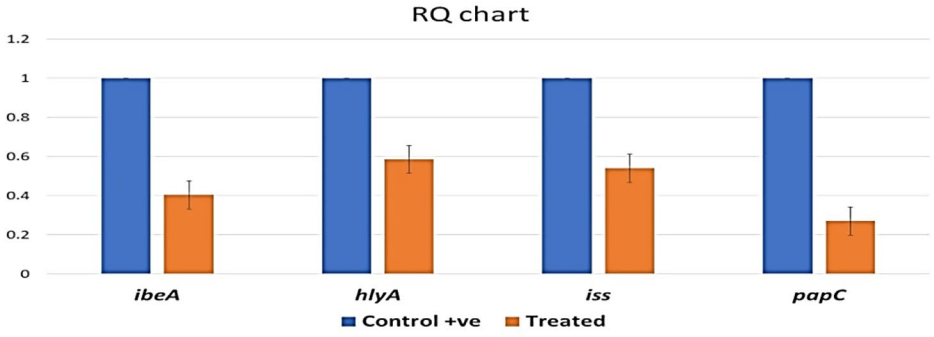

Fig. 7 Results of expression and fold change values of target virulence genes in *E. coli* samples of that treated with AG-CuNPs in relation to the genes in control non-treated sample by RTQ – PCR showed a significant difference in all of these detected genes

Table 4 Effect of AG-Cu NPs on some serum biochemical parameters

G	Periods	Total protein (g/dl)	Albumin (g/dl)	Globulin (g/dl)	ALT (u/l)	GGT (u/l)	ALP (u/l)
G1	**PT**	3.83 ± 0.12 ^{c}	1.54 ± 0.04 ^{b}	2.29 ± 0.08 ^{c}	52.95 ± 1.11 ^{a}	16.73 ± 0.51 ^{a}	61.29 ± 1.67 ^{a}
	AEE	4.07 ± 0.11 ^{bc}	1.70 ± 0.02 ^{b}	2.37 ± 0.11 ^{ab}	52.82 ± 0.86 ^{a}	16.91 ± 0.62 ^{a}	63.26 ± 1.92 ^{a}
G2	**PT**	3.22 ± 0.08 ^{a}	1.19 ± 0.06 ^{a}	2.02 ± 0.02 ^{a}	63.36 ± 0.91 ^{c}	21.33 ± 0.86 ^{c}	70.36 ± 0.73 ^{c}
	AEE	3.55 ± 0.07 ^{a}	1.46 ± 0.04 ^{a}	2.09 ± 0.04 ^{a}	58.71 ± 0.69 ^{b}	20.56 ± 0.42 ^{c}	68.71 ± 0.81 ^{b}
G3	**PT**	3.75 ± 0.06 ^{bc}	1.52 ± 0.04 ^{b}	2.23 ± 0.03 ^{bc}	57.45 ± 0.74 ^{b}	18.49 ± 0.44 ^{ab}	63.49 ± 0.95 ^{ab}
	AEE	4.21 ± 0.10 ^{c}	1.73 ± 0.04 ^{b}	2.49 ± 0.09 ^{b}	54.45 ± 1.30 ^{a}	17.22 ± 0.44 ^{ab}	62.00 ± 0.40 ^{a}
G4	**PT**	3.55 ± 0.04 ^{b}	1.44 ± 0.06 ^{b}	2.11 ± 0.05 ^{ab}	56.19 ± 0.65 ^{b}	19.80 ± 0.81 ^{bc}	65.82 ± 1.12 ^{b}
	AEE	3.91 ± 0.03 ^{b}	1.73 ± 0.05 ^{b}	2.18 ± 0.02 ^{a}	53.18 ± 0.80 ^{a}	18.61 ± 0.39 ^{b}	62.49 ± 0.47 ^{a}

The various letters in the same colon of the same period indicate statistically significant differences when (P < 0.05). G1 = negative control, G2 = infected control, G3 = noninfected + AG-CuNPs, G4 = infected + AG-CuNPs, PT = Post treatment, AEE = At experimental end (Mean ± SE) n = 5

Table 5 Effect of AG-Cu NPs on lysozyme activity, C reactive protein, uric acid and creatinine

G	Periods	Lysozyme activity (µMol)	C reactive protein (mg/l)	Uric acid (mg/dl)	Creatinine (mg/dl)
G1	**PT**	120.61 ± 1.93 ^{b}	4.98 ± 0.11 ^{b}	5.91 ± 0.25 ^{a}	0.43 ± 0.01 ^{a}
	AEE	122.41 ± 1.52 ^{b}	4.09 ± 0.22 ^{b}	5.87 ± 0.07 ^{a}	0.51 ± 0.01 ^{a}
G2	**PT**	107.80 ± 1.66 ^{a}	28.11 ± 0.41 ^{d}	7.18 ± 0.19 ^{b}	0.56 ± 0.02 ^{c}
	AEE	112.46 ± 1.80 ^{a}	14.21 ± 0.26 ^{c}	6.88 ± 0.20 ^{b}	0.58 ± 0.01 ^{b}
G3	**PT**	132.99 ± 1.59 ^{c}	4.01 ± 0.09 ^{a}	6.10 ± 0.38 ^{a}	0.44 ± 0.02 ^{ab}
	AEE	126.93 ± 1.81 ^{b}	3.07 ± 0.04 ^{a}	5.52 ± 0.25 ^{a}	0.52 ± 0.01 ^{a}
G4	**PT**	129.11 ± 1.65 ^{c}	10.22 ± 0.28 ^{c}	6.63 ± 0.32 ^{ab}	0.49 ± 0.01 ^{b}
	AEE	125.89 ± 1.27 ^{b}	4.08 ± 0.05 ^{b}	5.66 ± 0.37 ^{a}	0.51 ± 0.02 ^{a}

The various letters in the same colon of the same period indicate statistically significant differences when (P < 0.05). G1 = negative control, G2 = infected control, G3 = noninfected + AG-CuNPs, G4 = infected + AG-CuNPs, PT = Post treatment, AEE = At experimental end (Mean ± SE) n = 5

Table 6 Effect of AG-Cu NPs on copper (Cu) residues in liver and muscle

Periods	G	G1	G2	G3	G4
After treatment	**Liver Cu (mg/kg)**	1.71 ± 0.02 [a]	2.09 ± 0.05 [b]	2.26 ± 0.04 [b]	3.10 ± 0.13 [c]
	Muscle Cu (mg/kg)	0.24 ± 0.00 [a]	0.24 ± 0.01 [a]	0.27 ± 0.00 [b]	0.33 ± 0.00 [c]
At the end of the experiment	**Liver Cu (mg/kg)**	1.49 ± 0.02 [a]	1.59 ± 0.03 [a]	1.80 ± 0.02 [b]	2.45 ± 0.05 [c]
	Muscle Cu (mg/kg)	0.20 ± 0.00 [b]	0.23 ± 0.01 [c]	0.18 ± 0.00 [b]	0.20 ± 0.00 [b]

The various letters in the same row of the same period and organ indicate statistically significant differences when ($P < 0.05$). G1 = negative control, G2 = infected control, G3 = noninfected + AG-CuNPs, G4 = infected + AG-CuNPs, PT = Post treatment, AEE = At experimental end (Mean ± SE) n = 5

synthesized AG-CuNPs as an antibiotic alternative were used besides analyzing their effects *in-vivo* against *E. coli* O17 infection in broilers on clinical signs, *E. coli* re-isolation and count, immune status, anti-inflammatory activity, liver and kidney biomarkers, and muscle and liver tissues residues.

APEC, the main causal agent of colibacillosis in poultry farms, can induce enteric and extraintestinal infections in a syndrome associated with diarrhea and/or enteritis [45, 46]. APEC can colonize the intestinal and respiratory tracts of chickens [47]. Hussain et al., [48] isolated APEC from fecal samples of broilers showing signs of colibacillosis. As well, Saha et al., [49] reported that broiler droppings had the highest amount of APEC isolates (33.33%) followed by liver (19.54%). Abd El Tawab et al., [50] isolated APEC with higher rates of isolation from intestine (31.3%), liver (28.1%) followed by other organs. In the present study, *E. coli* was isolated from diseased broilers with an average incidence rate of 20%. Our results are nearly parallel to the results obtained by El-Seedy et al. [51], who reported a prevalence rate of 23%, while Hasan et al. [52] stated a rate of 29%. A high prevalence rate from diseased broilers (37.1%) was recorded by Abd El Tawab et al. [53], while Bushen et al. [54] recovered *E. coli* from broiler-dropping samples with an incidence rate of 39.0%. Differences in the isolation rate of *E. coli* may be due to early therapeutic and prophylactic use of antibiotics, the immune status of broiler chickens on the farm, hygienic measures, and management on the farm. Our serological typing study of *E. coli* isolates revealed that the examined samples belonged to O17: H18, O121: H7, O78, O127: H6, O91: H21, O103: H2, and O159. Serotype O78 was the most prevalent, with 30%, followed by O91: H21 with 20%, followed by O17: H18 with 18%. O17 was isolated and detected only in liver samples; O78 and O91 were isolated from liver and intestinal samples, while O121 and O159 were isolated from intestinal samples. A similar study by Younis et al. [55] reported the isolation ofO78 and O127 from broiler colibacillosis. Additionally, Amer et al. [56] recovered O78, O86, O158, O127, O91, O25, and O119, while Ibrahim et al. [57] detected other serotypes as O1,O2, O9, O18, O25, O26, O78, O111, O114, O119, and O127 from broiler chicken. Differences in the serotypes distribution may be due to variations in the time of sample collection and isolation, depending on the variation of isolation area.

The pathogenicity of APEC strains is related to the expression of several putative virulence genes (Table 2). Outer membrane protease (*ompA*) and increased serum survival (*iss*) are associated with protecting/serum resistance genes responsible for resistance to innate immunity and increased survival activity of bacteria in host serum. *ibeA* is functional for cell invasion into the host tissues, Hemolysin A (*hlyA*) creates pores in membranes of host cells (cell lysis), while fimbrilar *papC* (pyelonephritis associated Pili) gene stimulates the production of cytokines by T lymphocytes and colonization factor in extraintestinal infections [58]. In the present study, PCR detection and amplification of five virulence genes including (*ibeA, hlyA, iss, papC and ompA*) that represent and constitute different mechanisms of virulence in the majority of APEC strains revealed that*hlyA* gene was the most frequently expressed in all serotyped isolates (O17, O78, O91, O103, and O159) of APEC followed by *iss* and *papC* genes which were found in serotyped strains O17, O78, and O121, while *ibeA* gene was amplified and detected only in serotype O17. The *OmpA* gene is not detected in any strain serotypes. Invasions of microbes into the host tissues are essential in encouraging entry through the initial stage of infection [58]. Multiple genes encode invasions such as *ibeA* [59]. Regarding the detection of *ibeA* virulence gene markers in APEC serotyped isolates, only in serotype O17, Obata-Yasuoka et al. [60] reported that the occurrence of *ibeA* in APEC strains was 26%. Furthermore, Germon et al. [61] concluded that *ibeA* is positively associated with some strains of APEC, such as O88, O18, and O2 strains, while it was negatively associated with O78 strains. Hemolysin (*hly*) is a toxin responsible for cytotoxic activity in APEC. In our study, *hlyA* was detected with a rate of 100% in all serotypes of APEC isolates. A similar result in Egypt by Sedeek et al. [62] demonstrated that the virulence gene hemolysin *hlyF* was detected at a rate of 100% in all APEC isolates (O78a, O1, O26, and O78b), while Knopl et al. [63] reported that the occurrence of *hly in* APEC was (34%) and in another study by Johnson et al. [64] the incidence of *hlyF* in APEC was 78.2%. Another study in Egypt by Helal, [65] reported that the *iss* gene is APEC's most significant and frequently distributed virulence marker.

Moreover, Wilczynski et al. [66] showed that *the iss gene was APEC's most frequently amplified gene*. Regarding ompA in our study, it was not detected in any isolated *E. coli*, while De Carli et al. [67] recorded 100% of *ompT* within the APEC strains. Mohamed et al. [68] recorded *iss* and *papC* in APEC isolated from broilers. Furthermore, Abd El-Tawab et al. [69] recorded *iss* and *ompA* in broiler chicken in Egypt. Detection and amplification of these virulence genes in APEC strains may differ according to the geographic region and season or year of the isolation.

Regarding serogroup O17 isolated in our study, it was isolated from liver samples of broilers with colibacillosis, and it comprised four virulence genes (*ibeA, hlyA, iss*, and *papC*). Previous results by Ananias and Yano [70] stated that systemic infection of O17 was isolated from patients with sepsis and reported that 100% of the O17 strains harbored *papC*. It was previously detected as Shiga toxin-producing *E. coli* [71] and isolated from the meat of chicken [72]. Furthermore, it is isolated from farmed poultry by Samanta et al. [73]. O17 exposed multi-drug resistance and has been responsible for more severe systemic infections in humans, including the urinary tract [74], and it was linked to nonhuman reservoirs, mostly chicken and pork [75].

In our study, AG-Cu and ZnNPs were synthesized by a green method using Arabic gum as stabilizing and capping agents. NPs can be synthesized using chemical methods such as chemical precipitation [76] or physical methods, sonochemical, solvothermal, sol-gel process, and hydrothermal decomposition [77]. All these methods need either expensive instruments or complicated techniques or have potentially hazardous effects on the environment, especially in the case of large-scale production of NPs [78]. Recently, the green synthesis of the nanoparticle has been an incipient phenomenon that effectively reduces environmental risk by eradicating the hazardous components that are harmful to human health [79]. Surface modification of NPs is necessary to control morphological characters, especially size, to optimize their efficacy in addition to controlling the state of agglomeration, which hinders the application of NPs, especially as antimicrobials [80] and keeping electrostatic interactions and steric hindrance of NPs in water system depending on the polyanionic nature of Arabic gum [81].

Here, this study uses Arabic gum as stabilizing and capping agent with a ratio of 1 and 1.5% in addition to L- ascorbic acid and sodium hydroxide as precipitating agents in the case of AG-Cu and Zn NPs synthesis, respectively. Arabic gum exudates have hydrocolloid and physical emulsification properties and a complex mixture of polysaccharides and glycoprotein, so it is considered multi-functional material with good stabilizing properties and biocompatibility with non-toxic and safe nature [82]. Our method successfully synthesized AG-Cu and Zn NPs in sizes of 58 and 75 nm, respectively, with a narrow size distribution (PDI) of 0.16 and 0.15, respectively. Surface charge of -24.8 and −25.5 mV (Fig. 2; A1 and A2) respectively by Zetasizer, which was confirmed by TEM (Fig. 3; A1, 2 and B1, 2) that showed distinctive single well-dispersed NPs with a spherical shape, and without aggregation, and their size ranged from 7.68 to 19.5 nm for CuNPs and from 23.4 to 39.6 nm for ZnNPs. There is a direct relationship between the amount of added Arabic gum and the size of NPs resulting from aggregation in the case of increasing Arabic gum percent [83]. It was mentioned that a lower amount of Arabic gum helps in covering ZnNPs with a thin layer and allowing little particles to adhere together during the growth step when NPs bond with functional groups of Arabic gum such as carboxyl, hydroxyl, and amine groups, leading to avoiding the excess growth [83]. Moreover, 1% of Arabic gum can transform the charge dispersal of CuNPs, directly affecting the nucleation and monodispersed nature of CuNPs [27]. Nanoparticles synthesized in the presence of Arabic gum as stabilizing agents usually have negative charges on their surface resulting from the interaction of arabinogalactan proteins of AG with polysaccharide constituents that expand into the aqueous solution, giving electrostatic stability [27].

The XRD pattern of the AG-Cu and ZnNPs (Fig. 2; B1 and B2) revealed characteristic peaks (marked by red) of the metallic cubic and hexagonal phase of Cu and Zn NPs, respectively, corresponding to 2θ values of 43.3, 50.4, 74.1, 89.9, and 95.1° for CuNPs and 18.81, 32.34, 38.15, 50.86, 57.68, 61.23, 68.64, and 70.96°for ZnNPs at a wavelength of 1.54060corresponding to reference code (COD-9,012,043) for CuNPs as mentioned by Otte, [84] and (COD-1,529,590) for ZnNPs as mentioned by Baneeva and Popova, [85].

The role of Arabic gum in the synthesis of Cu and Zn NPs was identified by comparing the FT-IR spectra (Fig. 2; C1 andC2) of Arabic gum as stabilizing and capping agent with AG-Cu and Zn NPs. For Arabic gum, specific peaks of the N-H bond in stretching mode, O-H bond in stretching mode, N-H bond which bent in primary amine, and C-O bond in the stretching mode were observed at 3433, 2923, 1614, and 1070 cm^{-1}, respectively compared with 3430, 2918, 1627 and 1036 cm^{-1} for AG-CuNPs and 3431, 2920, 1630 and 1118 cm^{-1}, respectively for AG-ZnNPs. The shifting in the peak of the N-H bond in the stretching mode of AG stabilized NPs compared with AG may be resulted from an interaction between AG protein and NPs [26]. The shifting in the peak of the C-O bond in the stretching mode of AG stabilized NPs compared with AG indicates new bond formation, and as it was reported by Geetha et al., [26], the higher shifting frequency indicates structural changes

related to binding between AG and NPs. FT-IR study results confirmed that Arabic gum's role in stabilizing Cu and Zn NPs was successfully achieved.

Different decisive factors impact the cytotoxicity of NPs, especially shape, surface charge, size, surface modification and stabilization, and time-dose dependent effect. Therefore, nanoparticle characteristics like morphology, surface charge, size, chemical structure, and agglomeration state should be considered before cytotoxicity or *in-vivo* experimentation [86]. The most commonly mentioned theoretical mechanisms in the literature are: firstly, metal ions uptake (translocation and particle internalization) into cells, followed by a decline of intracellular ATP production and interruption of DNA replication [87]; secondly, production of reactive oxygen species (ROS) from metal NPs and metal ions, with subsequent oxidative damage to cellular structures [88];and finally, accumulation and dissolving of metal NPs in the bacterial cell causing the disturbance in permeability and cellular components [89]. For CuNPs, the cytotoxicity is mainly related to oxidative stress either directly by activation of ROS generation, mainly superoxide, hydroxyl, and hydrogen peroxide free radicals, or indirectly by stimulating the cell redox system causing ROS to release, which damages cellular components, mainly DNA causing oxidative DNA damage and genotoxicity [86]. For ZnNPs, the primary mechanism of its cytotoxicity is the induction of oxidative stress [90] and free radicals generation. Our results revealed that the survival rate of OEC cell culture incubated with AG-stabilized CuNPs with different concentrations decreased from 98.7 to 81.25% at concentrations of 0.31 and 50 mg/ml, respectively. For AG-ZnNPs, the survival rate decreased from 101.82 to 89.23% at concentrations of 0.31 and 50 mg/ml (Fig. 3C). The relationship between the surface functionalization of NPs using capping agents and nano cytotoxicity is closely related. It was reported that long-chain capping agents could reduce ROS generation and inhibit cytotoxicity even at high concentrations [91]. Arabic Gum, as a long-chain polysaccharide used as a capping and stabilizing agent in the synthesis of Cu and Zn NPs, helps in reducing cytotoxicity in a high concentration of less than 50 mg/ml due to controlling free radicals production, NPs redox potential, sharing in catalytic cycle and subsequently toxic components production [92].

AST of commercial antibiotics or AG-ZnNPs indicated the complete resistance of all of the tested *E. coli* strains; O17, O78, O91, O121, and O159, to six antibiotics; amoxiclav, cefotaxime, gentamicin, doxycycline, sulphamethoxazole-trimethoprim (cotrimoxazole), and enrofloxacin from six different families besides all AG-ZnNPs concentrations (Fig. 4; A-C). However, AG-stabilized CuNPs have to ascend antimicrobial efficacy against the tested isolates at all concentrations from 20 to 100 mg/ml (Table 3), where its IZDs are considered effective as commercial regular used antimicrobials. The *E. coli* O17 strain used in our *in-vivo* study showed that the highest IZD ranged from 19.66±0.33 to 25.00±0.00 mm, corresponding to the used concentration. MIC and MBC of AG-Cu NPs varied according to the *E. coli* tested strains. MIC values ranged from 3.75 to 15 mg/ml, while the bactericidal effect of AG-Cu NPs (MBC) was 60 mg/ml for O17, O78, and O121; other O91 and O159 required higher concentrations than 60 mg/ml. Several concerns have been raised about the emergence of multiple antibiotic resistance (MAR) pathogens due to the heavy and random use of some of the most commonly used antimicrobials in poultry farms as the first choice for bacterial infection treatment. The responsible use of antibiotics should be adopted, and alternative antimicrobial agents with more potent immune-stimulatory properties necessary to combat *E. coli* infection should be applied besides routine monitoring of drug susceptibility patterns overtime to avoid antibiotics resistant mutants. In literature, AST of various isolated avian *E. coli* serotypes from colibacillosis cases of broilers outlined different percentages of resistance and sensitivity due to strain differences. Similarly, Ramchandani et al. [93] reported that 56% of human-associated multidrug-resistant uropathogenic *E. coli* were O17, which has an animal origin from 24 chicken samples, were resistant to trimethoprim-sulfamethoxazole, ampicillin, ciprofloxacin, amoxicillin/clavulanic acid, tetracycline, chloramphenicol, gentamicin, cephalothin, streptomycin, and kanamycin. Our antibiogram-resistant results related to some extent with Adam et al. [1], where some *E. coli* isolates were highly resistant (75%) to 9 out of 12 different tested antibiotics. Isolates revealed resistance to cephalothin, lincomycin,and erythromycin (100%), doxycycline (60%), amoxiclav(40%), and enrofloxacin, neomycin, streptomycin, and tetracycline (20%). Massot et al. [94] found that 44.8% of the collected strains showed one or more antibiotic resistances among the ten tested ones (penicillins, cephalosporins, carbapenems, aminoglycosides, tetracyclines, sulfonamides, amphenicols, quinolones, phosphonic acid, and furans). In comparison, 2.2% of all strains were multi-resistant to at least penicillins, cotrimoxazole, and quinolones.

Concerning our NPs antibiogram, Abdollahi et al. [95] recorded that antimicrobial activity IZDs of CuNPs against *E. coli* among other pathogens ranged from 20 to 32 mm. Moreover, the high *in-vitro* bactericidal efficiency of CuNPs against *E. coli* was recorded [96, 97]. Lower MIC 120 and MBC 160 µg/ml of cupric oxide NPs for *E. coli* were recorded by Chakraborty et al. [98]. For CuNPs, Su et al. [99] reported that its intracellular penetration caused a significant alteration of bacterial key protein expressions followed by a significant alteration in the metabolic growth processes. Radi et al. [100]

evidenced the antibacterial activity of ZnNPs against *E. coli*. The difference in our antibacterial susceptibility between AG-Cu and Zn NPs stabilized by the Arabic gum may be attributed to their different NPs size, which could limit the entrance and the non-specific transport across the bacterial cell membrane [101].

Furthermore, Azam et al. [102] clarified that the antimicrobial activity of ZnNPs increased against gram-negative bacteria by decreasing their particle size. Hence, AG-CuNPs are more effective against *E. coli* variant strains than AG-ZnNPs. The smaller the NPs, the larger the surface area and surface reactivity, and subsequently, the high production of hydrogen peroxide free radicals due to a high number of NPs per unit volume [103], causing inhibition of *E. coli* bacterial growth. It was reported that the small size of AG-ZnNPs at 16 nm and AG-CuNPs at 12 nm have the highest antibacterial efficacy against *E. coli* bacteria due to high hydrogen peroxide free radicals generation causing bacterial damage [83].

TEM analysis of thin sections prepared from E. coli O17 cultures after treatment with 50 mg/ml AG-CuNPs (Fig. 5; A-F) revealed anchoring and accumulating NPs around the bacterial cell wall with bacterial cell deformity and elongation. Additionally, it showed intracellular distribution in the cytoplasm with a ghostly appearance devoid of cytoplasmic content, a destabilization of the cellular membrane resulting in low electronic density, a faint appearance of cytoplasm, and cell damage. These findings are similar to those explained by Díaz-Visurraga et al. [104], who showed that the first interaction of metal NPs with the cell wall results in exopolysaccharide matrix fragmentation, cell separation, elongation, and cell reorganization into small clusters. These modifications enhance the surfaces of physically interacting bacterial cells with nanostructured materials. Ghost formation seems to be another morphological feature related to the NPs toxicity in bacterial cells. Indeed, a cell ghost is an intact surface structure lacking cytoplasmic content, including DNA mainly from gram-negative bacteria, but not always. The deformity of the cell's physical structure may cause the membrane to swell and disturb, increasing membrane fluidity, which in turn raises passive permeability and demonstrates as leakage of various critical intracellular constituents like ATP, DNA, sugar content, enzymes, and amino acids [104].

Antibacterial performance assay of AG-CuNPs on *E. coli* O17 (Fig. 6; A and B) displayed the effect of different (*E. coli*-AG-CuNPs) contact time and AG-CuNPs concentrations on the viability of *E. coli* O17 to meet the bactericidal activity threshold. It was found to be increased with prolonged time and higher concentrations. The antibacterial rate reached 100%, at 20 min and 40 mg/ml AG-CuNPs. Other literature reported that the antibacterial effect of CuNPs against *E. coli* is complementary action dependent on the concentration of NPs. A higher concentration will be more effective, where a large surface area to volume ratio helps in bacterial cell wall damage and cell death [105]. Besides the sudden decline in membrane integrity, the release of ROS contributes to the degradation of several biomolecules that affect normal cell viability [106]. Compared to other studies, our time-kill and concentration results varied from that of Li et al. [33], who reported that antibacterial efficiency reached nearly 100% after 28 min at 4.0 g/L CuNPs, while Du et al. [107] recorded it after 4 h exposure at 500 mg/l and40 nm. These discrepancies are possibly attributable to the variation in NPs size, *E. coli* strain, and the synthetic method used.

E. coli O17 serotype has been used for experimental broiler challenge and to evaluate the effect of AG-CuNPs on these virulence genes because it is the highest strain in the number of detected virulence genes (4 genes). In this study, the qRT-PCR was used to investigate the frequency and fold change of the virulence genes in the APEC O17 strain before and after treatment with AG-CuNPs. Our study explored that virulence genes (*ibeA, hlyA, iss*, and *papC*) were significantly down regulated in the treated *E. coli* strain sample compared to the control non-treated strain after the treatment dose of AG-CuNPs (50 mg/ml) (Fig. 7). A similar result was reported; CuNPs, compared with silver NPs, were more effective on the *E. coli* genome [108]. Another study by Awaad et al. [109] demonstrated that silver NPs down regulated *iss, papC, iutA, iron*, and *fimH* virulence genes expression.

Our study recorded negative impacts post virulent *E. coli* O17 infection, such as severe retardation in growth, feed intake, organs' lesion score, and mortalities; similar findings were reported by Rosa et al. [110]. On the other hand, treated group G4 had no mortality with a general improvement in broilers' activity that may be attributed mainly to the curative antibacterial activity of the used NPs on pathogenic *E. coli* or its virulence genes. As well, El-kazaz and Hafez [111] observed the positive effect of CuNPs on all broilers' behavioral patterns (feeding, drinking, crouching, resting, and movement) post their addition to drinking water (10 mg/l) for five weeks, attributing these results to the significant reduction of serum corticosterone values which might indicate an inhibition of the stress condition. Moreover, Sarvestany et al. [112] found that even at a dose of 100 mg/kg, CuNPs had no adverse effects when used as an alternative to antibiotics in poultry.

Our results displayed that *E. coli* re-isolation and count were markedly decreased in infected treated G4 compared to infected control G2 in its intestinal count. At the same time, no *E. coli* was re-isolated from liver samples, which assured the efficacy of AG-CuNPs in stopping the systemic infection of *E. coli* O17 *in-vivo*. Our *in-vivo*

findings are long-established with our antibacterial activity regarding *in-vitro* tests and TEM analysis. Similarly, Hassanen et al. [7] found that oral doses of CuNPs 5 mg/kg body weight for seven days reduced 50% of *E. coli* O78 count in blood, liver, and other organs than challenged untreated broilers. Hence, CuNPs could penetrate the intestinal walls, where smaller constituent parts can diffuse faster through the GIT mucus to directly enter the bloodstream, after that being pre-dominantly scavenged by the liver and spleen [113].

Our results showed a significant decrease in TP, albumin, globulin, and lysozyme activity besides an increase in C-reactive protein, ALT, GGT, and ALP activities, uric acid, and creatinine in infected control G2 than control G1 (Tables 4 and 5). Post-treatment, non-infected treated G3 revealed no significant difference than G1 in TP, albumin, globulin, uric acid, or creatinine, while significantly decreased C-reactive protein levels and increased lysozyme activity and most of the activities of the detected enzymes; at the end of the experiment results mostly returned to its normal levels. Infected treated G4 showed a significant improvement in most of the detected parameters than G2 by increasing TP, albumin, globulin, and lysozyme activity besides decreasing C-reactive protein, uric acid, creatinine, and most of the activities of the detected enzyme than G2. In contrast, it showed no significant difference from G1 in most of these detected parameters at the end of the experiment. Concerning changes in liver biomarkers, proteins are considered the terminal executors of specific biological processes, such as catalyzing metabolic reactions and transporting substances [99], while ALT and GGT values are considered two proper hepatic function evaluation tests; hence, an increase in their activities is indicative to hepatocellular injury [114].

Moreover, Balakrishna and Prabhune [115] mentioned that GGTs are highly conserved enzymes that play an essential role in glutathione homeostasis (a major cellular antioxidant) due to some of the common physiological γ-glutamyl substrates like glutathione. Regarding G2, the detected virulence genes of *E. coli* O17 confirmed its systemic *in-vivo* consequences on vital organs. Manafi et al. [116] reported a similar increase in ALT, and ALP, attributing these influences to *E. coli* endotoxins that passed through the intestinal wall to the blood, causing consequent damage to liver and kidney organs, which appeared as severe to moderate pathological alterations as found by Hassanen et al. [7].

Our findings of treated groups G3 and G4 indicated an immune stimulant effect of AG-CuNPs without enduring adverse effects on liver or kidney functions. These *in-vivo* findings coincided with our previous cytotoxicity assay. Hence, AG-CuNPs suppress the progressive destructive effects of *E. coli* through their effective antibacterial activity on the bacteria or its virulence genes. Compared with other studies, El-Kassas et al. [117] recorded that CuNPs reduce liver enzyme activities, protect the hepatic tissue from degenerative changes, and increase stress resistance. Moreover, Sizova et al. [103] found that CuNPs tended to increase serum TP and aminotransferase activities without changes in GGT, lactate dehydrogenase (LDH) activities, or liver microstructure of treated groups. The authors considered GGT as a marker of amino acid balance and assumed that the increase in ALT activity indicates changes in the metabolic flows of the NPs-treated groups. Hence, the effect on enzyme activity depends on NPs absorption and metabolism according to their physicochemical properties, such as size, shape, surface chemistry and charge, length, method of administration, and dose [118].

Consequently, the benefits or drawbacks of NPs on vital organs, redox reactions, and immune defense depend mainly on selecting their effective, safe dose. For example, Abdelazeim et al. [119] and Elkhateeb et al. [120] reported that high continuous daily doses of CuNPs (100 and 250 mg/kg body weight, respectively) are required to induce toxicity of the liver or kidney. On the other hand, Cholewińska et al. [121] reported that low doses of dietary CuNPs cause a significant increase in plasma AST, ALT, and ALP activities, while they decrease ALT activities at high doses. Conversely, Morsy et al. [106] observed that 15 mg/ml CuNPs revealed a remarkable improvement in the treated *E. coli*-infected broilers; it caused some pathological alterations in different organs with high Cu levels in the liver and kidneys. Other studies revealed that CuNPs reduced the level of albumin in chickens [122]; meanwhile, Scott et al. [123] found a significant decrease in ALT, AST, and uric acid levels by 20 mg/kg CuNPs and a non-significant effect on albumin, ALP, and LDH.

The present study demonstrated a significant increase in lysozyme activity of both treated groups G3 and G4 than G1 and G2 (Table 5). Elevation of serum lysozyme is a good indicator of immune system activation besides its antimicrobial mechanism. It is released from mononuclear phagocytes, which are involved in disease resistance, especially during infection. Furthermore, Lysosomes play an essential role in degrading dysfunctional proteins and damaged organelles to maintain cellular homeostasis. Besides, they are mainly involved in receiving and degrading phagocytized macromolecules [124]. Similar results were reported by El-Kassas et al. [117] besides the CuNPs' effect on upregulating immune-modulatory genes. Besides, Arancibia et al. [125] observed that CuNPs recruit different innate immune cells, such as macrophages and neutrophils, which are crucial to initiating the immune response to different foreign molecules or harmful agents.

Moreover, the redox-active properties of MONPs tend to modulate the innate and adaptive immunity that successfully enhances the immune response [126]. The perspective of CuNPs as an immune-modulator is promising for their future use in poultry feed and medicine [13]. In contrast, lysozyme activity post-CuNPs supplementation was non-significantly changed in the previous study by El-kazaz and Hafez [111].

C-reactive protein (CRP) is γ-globulin produced by the liver and classified as an acute phase reactant, which means that it rises in response to general inflammation, infection, or tissue injury following IL-6 secretion by macrophages. It is produced in various bacterial diseases because it acts as an opsonin that helps in complement activation and has a receptor on phagocytic cells besides binding to the bacterial lysophosphatidyl choline [127]. Therefore, enhancing pro-inflammatory cytokines (CRP, IL-6, and ceruloplasmin) is vital for restoring homeostasis to normal physiological ranges [128]. However, in the inflammatory phase, ROS can damage the proteins and DNAs. Hence, the anti-inflammatory properties of AG-CuNPs (Table 5) that significantly decreased CRP levels positively impact counteracting infection subsequences, supporting vital organ functions and general health aspects besides its antibacterial activity. Similar anti-inflammatory properties and inhibition of other inflammatory markers and tissue damage by CuNPs were reported by El-kazaz and Hafez [111], El-Kassas et al. [117], and Faisal et al. [129].

Regarding the kidney biomarkers (Table 5), increased serum creatinine and blood urea nitrogen concentrations impaired renal function and thereby decreased glomerular filtration rate due to creatinine being freely filtered in kidney glomeruli and typically no tubular re-absorption [130]. Scott et al. [123] revealed that the participation of CuNPs leads to decreasing blood urea, indicating its potential association with higher protein metabolism/formation and more efficient utilization of amino acids for growth. In general, the varied and sometimes contradictory results for the effect of CuNPs on biochemical markers can be explained by variations in routes of administration, treatment dose, and duration, besides differences in NPs physicochemical properties that induced different biological reactions.

Results of Cu residues (Table 6) indicated that *E. coli* infection significantly increased Cu residues in G2 than G1 and in infected treated G4 than in non-infected treated G3. Although, in general, Cu residues in the liver were more than in muscle, all Cu levels decreased by time at the study end with no significant difference than G1 in muscles, while it needs more time to decrease in the liver organ. The absence of metal residues at the end of the study assured that small-size NPs from the lymphatic and circulatory systems might distribute to organs, including the kidneys, from where they can be rapidly cleared [113], which was assessed in our AG-CuNPs characters.

Furthermore, Cholewińska et al. [121] mentioned that hepatic Kupffer cells are of paramount importance in NPs elimination; tiny ones are filtered out of the liver through the kidneys, but bigger ones are retained in the Kupffer cells. Similarly, Sizova et al. [103] and Morsy et al. [106] detected the highest Cu content in liver tissue and the lowest in muscle. The high hepatic accumulation of MONPs may be due to the high production rate of metallothioneins (MTs) which ultimately bind the metals to avoid possible harm [131]. Moreover, the liver is a specialized organ for metal detoxification and Cu metabolism through metal sulfur-protein formation. Meanwhile, the less concentration of MONPs in the muscle may be due to the low level of metal-binding protein as MTs in the muscle and owing to the large mass with the low metabolic activity of muscular tissues [132]. The biocompatibility and toxicity of MONPs are essential criteria to take into account for their biomedical applications. Their biocompatibility is linked to the biodegradation of metabolites and the immune system response post-administration. Their toxicity profile may be increased or decreased due to modifying their cell/tissue biodistribution and clearance/metabolization. Hence, the size and distribution, besides shape, are the crucial objects influencing the pharmacokinetics and biodistribution *in-vivo* applications and determining their fate.

Additionally, the surface charge plays a vital role in the physical stability and influences its interaction with the biological system and its safety. Similarly, Sawosz et al. [133] and El-Kassas et al. [117] found no change in Cu levels of breast muscle or liver to control post-feeding with CuNPs at 7.5 mg/kg or 100% of the daily requirement for 42 days, respectively. Moreover, Ognik et al. [134] showed that shortening the period of CuNPs administration to seven days decreased its accumulation. Furthermore, Ognik et al. [135] reported that once the level of Cu is too high, its absorption and accumulation probably decrease while its excretion increases to ensure normal metabolism. Besides, an additional increase of CuNPs than the recommended NRC amount showed no linear increase in the content of Cu in the liver or breast muscle [135]. On the contrary, Hassanen et al. [7] found a significant increase in Cu content in muscles with no significant difference in the liver. In addition, Sizova et al. [136] mentioned that CuNPs have high penetration ability through the intestines, bypassing traditional binding and transport by proteins, consequently giving a more consistent supply of Cu.

Conclusion

Multi-resistant *E. coli* strains have emerged as a serious worldwide problem. Most of the available antibiotics have lost their potency over *E. coli* due to their abuse, which could be found clearly in antibiogram tests. Hence, there is a growing trend to replace ineffective antimicrobials with alternative materials to intervene in a strategy for controlling bacterial infection in poultry farms. This study was designed to compare the efficiency of AG-Zn, and Cu NPs against various field-isolated APEC strains. AG-CuNPs were prepared through a green, eco-friendly, and safe method. From our results, we concluded that the morphology of AG-CuNPs showed smaller particle size and homogeneous distribution than AG-ZnNPs which signifies the antibacterial efficacy of Cu than Zn NPs against tested strains (O17, O78, O91, O121, and O159). Furthermore, the AG-CuNPs exhibited low cytotoxicity, efficient bactericidal activity at TEM, and antibacterial performance assays besides their anti-inflammatory and immune-modulator properties.

Moreover, it successfully decreased the expression of detected (*ibeA, hlyA, iss*, and *papC*) virulence genes of the *E. coli* O17 strain. Additionally, it neither affects liver or kidney functions nor leaves residues in muscles. It restored most of the tested biomarker levels to near the normal control values. Therefore, we highly recommend using AG-CuNPs as an alternative antibacterial agent (nanobiotic) in treating poultry-associated *E. coli* pathogens. AG-CuNPs have broad potential application prospects. Consequently, more studies are needed to compare their *in-vitro* and *in-vivo* effects against various economically critical bacterial infections of poultry production.

Supplementary Information

The online version contains supplementary material available at https://doi.org/10.1186/s12917-023-03643-y.

Additional file 1: Supplementary Fig. 1: A schematic illustration of the experimental design.

Additional file 2: Supplementary Fig. 2: Agarose gel electrophoresis for PCR amplification of hlyA virulence gene at (1177 bp) in APEC serotypes: Lane L (ladder), Lane + C (control positive), Lane - C (control negative), Lane 1 (serotype O17), Lane 2 (serotype O78), Lane 3 (serotype O91), Lane 4 serotype (O121) and Lane 5 (serotype O159). **Supplementary Fig. 3**: Agarose gel electrophoresis is for PCR amplification of ***ibeA*** virulence gene at **(342 bp)** in APEC serotypes: Lane L (ladder), Lane + C (control positive), Lane - C (control negative), Lane 1 (serotype O17), Lane 2 (serotype O78), Lane 3 (serotype O91), Lane 4 serotype (O121) and Lane 5 (serotype O159). **Supplementary Fig. 4**: Agarose gel electrophoresis for PCR amplification of ***iss*** virulence gene at **(309 bp)** in APEC serotypes: Lane L (ladder), Lane + C (control positive), Lane - C (control negative), Lane 1 (serotype O17), Lane 2 (serotype O78), Lane 3 (serotype O91), Lane 4 serotype (O121) and Lane 5 (serotype O159). **Supplementary Fig. 5**: Agarose gel electrophoresis for PCR amplification of ***papC*** virulence gene at **(200 bp)** in APEC serotypes: Lane L (ladder), Lane + C (control positive), Lane - C (control negative), Lane 1 (serotype O17), Lane 2 (serotype O78), Lane 3 (serotype O91), Lane 4 serotype (O121) and Lane 5 (serotype O159).

Acknowledgements
Not applicable.

Authors' contributions
Fawzia A. El-Shenawy: responsible for E. coli isolation and identification, serological typing, molecular detection of virulence genes by PCR, and detection of the efficacy of CuNPs on virulence genes by real-time quantitative PCR. Samr Kassem: responsible for preparation, characterization, TEM, and cytotoxicity assays of AG-ZnNPs and AG-CuNPs. Eman M. El. El-Sherbeny: responsible for performing MIC and MBC assay, blood and tissue sampling collection, estimating of liver and kidney function tests, anti-inflammatory C-reactive protein, immunomodulatory activity (globulin and lysozyme activity), and expressing serum biochemical test;as well, detecting Cu residues in liver and muscle tissues. Fawzia A. El-Shenawy and Eman M. El. El-Sherbeny: responsible for performing antimicrobial susceptibility test (AST) assay, the antibacterial performance of CuNPs, and E. coli count; responsible for following up the broiler's experiment. All authors are responsible for experimental design and writing this research paper.

Funding
This research received no specific grant from any funding agency in the public, commercial, or not-for-profit sectors.
Open access funding provided by The Science, Technology & Innovation Funding Authority (STDF) in cooperation with The Egyptian Knowledge Bank (EKB).

Data Availability
The corresponding author will provide the datasets used in this study on reasonable request.

Declarations

Ethics approval and consent to participate
The animal studies were approved by Research Ethics Committee for environmental and clinical studies (Protocol number: 165,429) at Animal Health Research Institute (AHRI) and were carried out following Egyptian Ethics Committee guidelines and the NIHGuidelines for the Care and Use of Laboratory Animals. In addition, all animal experiments were performed following the ARRIVE guidelines (https://arriveguidelines.org).

Consent for publication
Not applicable.

Competing interests
The authors declare no competing interests.

Author details
[1]Bacteriology unit, Tanta lab. (AHRI), Animal Health Research Institute, Agricultural Research Center (ARC), Giza, Egypt
[2]Pharmacology unit, Tanta lab. (AHRI), Animal Health Research Institute, Agricultural Research Center (ARC), Giza, Egypt
[3]Nanomaterials research and Synthesis unit, Animal Health Research Institute (AHRI), Agricultural Research Center (ARC), Giza, Egypt

Received: 25 September 2022 / Accepted: 12 July 2023
Published online: 04 August 2023

References

1. Adam AFH, Ismaael NA, Atiyahullah TMO, Bentaher ET, Gaidan OK, Meriz OM. Antibiotic susceptibility, serotyping and pathogenicity determination of avian *Escherichia coli* isolated from colibacillosis cases in broiler chicken in aljabel alakhdar region, Libya. Assiut Vet Med J. 2022;68:1–8.
2. Tivendale KA, Logue CM, Kariyawasam S, Jordan D, Hussein A, Li G, Wannemuehler Y, Nolan LK. Avian-pathogenic Escherichia coli strains are similar to neonatal meningitis *E. coli* strains and are able to cause meningitis in the rat model of human disease. Infect Immun. 2010;78:3412–9.
3. Nolan LK, Vaillancourt JP, Barbieri N, Logue CM. Colibacillosis. In: Swayne DE, Boulianne M, Logue CM, McDougald LR, Nair VL, Suarez DL, editors.

Diseases of Poultry.14th Edition. Hoboken: John Wiley and Sons, Inc; 2020. pp. 770–830.
4. Vandekerchove D, De Herdt P, Laevens H, Pasmans F. Colibacillosis in caged layer hens. Characteristics of the disease and the aetiological agent. Avian Pathol. 2004;33:117–25.
5. Radwan IA, Hassan HS, Abd-Alwanis SA, Yahia MA. Frequency ofsome virulence associated genes among multi drug-resistant *Escherichia coli* isolated from septicemic broiler chicken. Int J Adv Res. 2014;2:867–74.
6. Meena NS, Sahni YP, Thakur D, Singh RP. Applications of nanotechnology in veterinary therapeutics. J Entomol Zool Stud. 2018;6:167–75.
7. Hassanen EI, Morsy EA, HussienAM, Farroh KY, Ali ME. Comparative assessment of the bactericidal effect of nanoparticles of copper oxide, silver, and chitosan-silver against Escherichia coli infection in broilers. Biosci Rep. 2021;41:4.
8. Mohan AC, Renjanadevi B. Preparation of zinc oxide nanoparticles and its characterization using scanning electron microscopy (SEM) and x-ray diffraction (XRD). Proc Technol. 2016;24:761–6.
9. Bezza FA, Tichapondwa SM, Chirwa EMN. Fabrication of monodispersed copper oxide nanoparticles with potential application as antimicrobial agents. Sci. 2020;10:1–18.
10. Seil JT, Webster TJ. Antimicrobial applications of nanotechnology: methods and literature. Int J Nanomed. 2012;7:2767–81.
11. Kaviani EF, Naeemi AS, Salehzadeh A. Influence of copper oxide nanoparticle on hematology and plasma biochemistry of Caspian trout (Salmo trutta caspius), following acute and chronic exposure. Pollution. 2019;5:225–34.
12. ZhangZ, Chinnathambi A, Alharbi SA, BaiL. Copper oxide nanoparticles from Rabdosia rubescens attenuates the complete Freund's adjuvant (CFA) induced rheumatoid arthritis in rats via suppressing the inflammatory proteins COX-2/ PGE2. ArabJ Chem. 2020;13:5639–50.
13. SharifM, Rahman M, Ahmed B, Abbas RZ. HassanF. Copper nanoparticles as growth promoter, antioxidant and anti-bacterial agents in Poultry Nutrition: prospects and future implications. Biol Trace ElemRes. 2020;199:3825–36.
14. Lokina S, Narayanan V. Antimicrobial and anticancer activity of gold nanoparticles synthesized from grapes Fruit Extract. Chem Sci Trans. 2013;2:105–10.
15. Hussain Z, Khan JA, Anwar H, Andleeb N, Murtaza S, Ashar A, Arif I. Synthesis, characterization, and pharmacological evaluation of zinc oxide nanoparticles formulation. Toxicol Ind Health. 2018;34:753–63.
16. Quinn PJ, Markey BK, Carter ME, Donnelly WJC, Leonard FC. Veterinary microbiology and microbial diseases.1st Iowa. State University Press Blackwell Science; 2002.
17. GiovanardiD, Campagnari E, Ruffoni LS, Pesente P, Ortali G, Furlattini V. Avian pathogenic Escherichia coli transmission from broiler breeders to their progeny in an integrated poultry production chain. Avian Pathol. 2005;34:313–8.
18. Kok T, Worswich D, Gowans E. Some serological techniques for microbial and viral infections. In Practical Medical Microbiology Collee J., Fraser A., Marmion B. and Simmons, A., eds.), 14th ed., Edinburgh, Churchill Livingstone, UK. 1996.
19. EwersC LiG, Wilking H, KieblingS, AltK, Antáo EM, LaturnusC, Diehl I, Glodde S, Homeier T, Böhnke U, Steinrück H, Philipp HC, Wieler LH. Avian pathogenic, uropathogenic, and newborn meningitis-causing Escherichia coli: how closely related are they? Int J Med Microbiol. 2007;297:163–76.
20. Sambrook J, FritscghEF MentiatesTE. Molecular coloning. A laboratory manual. 2 ed. New York: Cold spring Harbor Laboratotry press; 1989.
21. Yamamoto S, Terai A, Yuri K, Kurazono H, Takeda Y, YoshidaO. Detection of urovirulence factors in Escherichia coli by multiplex polymerase chain reaction. FEMS MicrobiolImmunol. 1995;12:85–90.
22. Ewers C, Janßen T, Kießling S, Philipp HC, Wieler LH. Rapid Detection of Virulence-Associated genes in avian pathogenic Escherichia coli by Multiplex polymerase chain reaction. Avian Dis. 2005;49:269–73.
23. JohnsonJR SAL. Extended virulence genotypes of Escherichia coli strains from patients with Urosepsis in relation to phylogeny and host compromise. JInfect Dis. 2000;181:261–72.
24. MagrayMSUD, Kumar A, Rawat AK, Srivastava S. Identification of Escherichia coli through analysis of 16S rRNA and 16S-23S rRNA internal transcribed spacer region sequences. Bioinformation. 2011;6:370.
25. El-BoushyM, Awad E, Sanaa S, Hanfey A. Immunological, hematological and biochemical studies on pefloxacin in broilers infected with *E. coli*. 8th Conference, Vet MedZag. 2006:503–515.
26. Geetha A, Sakthivel R, Mallika J, Kannusamy R, Rajendran R. Green synthesis of antibacterial zinc oxide nanoparticles using biopolymer Azadirachtaindica gum. Orient JChem. 2016;32:955–63.
27. Chawla P, KumarN, Bains A, Dhull SB, Kumar M, Kaushik R, Punia S. Gum arabic capped copper nanoparticles: synthesis, characterization, and applications. Int J BiolMacromol. 2020;146:232–42.
28. Allam RM, Al-Abd AM, Khedr A, Sharaf OA, Nofal SM, Khalifa AE, Abdel-Naim AB. Fingolimod interrupts the cross talk between estrogen metabolism and sphingolipid metabolism within prostate cancer cells. Toxicol Lett. 2018;291:77–85.
29. EUCAST. European Committee on Antimicrobial Susceptibility Testing. Breakpoint tables for interpretation of MICs and zone diameters. 10, 2020. http://www.eucast.org.
30. Mohd Yusof H, Abdul Rahman N, Mohamad R, Hasanah Zaidan U, Samsudin AA. Antibacterial potential of Biosynthesized Zinc Oxide Nanoparticles against Poultry-Associated Foodborne Pathogens: an in Vitro Study. Animals. 2021;11:2093.
31. CLSI (Clinical and Laboratory Standars Institute). Performance Standards for Antimicrobial Susceptibility Testing, 30th ed. CLSI supplement M 100, Wayne, Pa, USA. 2020.
32. Liu Y, He L, Mustapha A, LiH, Hu ZQ, Lin M. Antibacterial activities of zinc oxide nanoparticles against Escherichia coli O157:H7. JAppl Microbiol. 2009;107:1193–201.
33. Li P, Lv W, Ai S. Green and gentle synthesis of Cu2O nanoparticles using lignin as reducing and capping reagent with antibacterial properties. J Exp Nanosci. 2016;11:18–27.
34. Yuan JS, Reed A, Chen F, Stewart CN. Statistical analysis of real-time PCR data. BMC Bioinform. 2006;7:85.
35. Reitman S, Frankel S. A colorimetric method for determination of serum glutamic oxaloacetic transaminase and serum glutamic pyruvic transaminase. Am J clin Path. 1957:25–65.
36. Szasz G, Weimann G, St ~ ihler F, Wahlefeld AW, Persijn JP. New substrates for measuring y-glutamyl transpeptidase activity. Clin Chem Clin Biochem. 1974;12:228.
37. Kind PRN, King EG. Colorimetric determination of alkaline phosphatase activity. J clin Pathol. 1954;7:322–35.
38. Gornall AG, BardawillCJ, David MM. Determination of serum protein by means of the biuret reagent. J Biol Chem. 1949;177:751.
39. Doumas BT, Watson WA, Biggs HG. Albumin standards and the measurement of serum albumin with bromocresol green. Clin Chim Acta. 1971;31:87–96.
40. Schltz LA. Veterinary haematology. Lea and Febiger. 1987;39:217–22. 3rd ed.
41. Macleod CM, Avery OTJ. Exper Med. 1950;73:191.
42. Fossati P, Prencipe L, Betri G. Colorimetric method for determination of serum uric acid. Clin Chem. 1980;26:227–73.
43. DI Giorgio J. Nonprotein nitrogenous constituents. In: clinical chemistry – principles and technics, 2nd ed. RJ Henry, DC Cannon, JW Winkelman, editors, Harper and Row, Hagerstown (MD), 1974; p. 541–553.
44. Okoye COB, Ibeto CN, Ihedioha JN. Assessment of heavy metals in chicken feeds sold in south eastern, Nigeria. Adv Appl Sci Res. 2011;2:63–8.
45. Jang, J.; Hur, H.G.; Sadowsky,M.J.; Byappanahalli,M.N.; Yan, T.; Ishii, S. Environmental Escherichia coli: Ecologyand public health implications—A review. J. Appl. Microbiol. 2017, 123, 570–581.
46. Solà-Ginés M, Cameron-Veas K, Badiola I, Dolz R, Majó N, Dahbi G, Viso S, Mora A, Blanco J, Piedra-Carrasco N, et al. Diversity of Multi-Drug resistant avian pathogenic Escherichia coli (APEC) causing outbreaks of colibacillosis in Broilers during 2012 in Spain. PLoS ONE. 2015;10:e0143191.
47. Dziva, F.; Stevens, M.P. Colibacillosis in poultry: Unravelling the molecular basis of virulence of avian pathogenic Escherichiacoli in their natural hosts. Avian Pathol. 2008, 37, 355–366.
48. Hussain H.L., Lqbal Z., Lqbal M., Kuang X., Wang Y., Yang L.,Lhsan A., Aqib A.I., Kaleem Q.M., Gu Y. and Hau H. Coexistence of virulence and β-lactamase genes in avian pathogenic Escherichia coli. Microbial Pathogenesis, 2022,163.
49. Saha O., Hoque N.M., Islam O. K., Rahaman M.M., Sultana M. and Hossain A.M. Multidrug-Resistant Avian Pathogenic Escherichia coli Strains and Association of Their Virulence Genes in Bangladesh. Microorganisms J., 2020, 8, 1135.
50. Abd El Tawab,A.A., Maarouf, A.A, Abd El Al, S.A., Fatma, I. E H and El Mougy,E.E.A. Detection of some virulence genes of Avian Pathogenic E. coli by polymerase chain reaction. Benha Veterinary Medical Journal, 2014, 26(2):159–176.
51. El-Seedy FR, Abed AH, Wafaa MMH, Bosila AS, Mwafy A. Antimicrobial resistance and molecular characterization of pathogenic *E. coli* isolated from chickens. J Vet Med Res. 2019;26:280–92.
52. Hasan HW, Abd El-Latife AAM, AbedHA. Bactriological and molecular studies on *E. coli* isolated from broiler chickens. Assiut Vet Med J. 2020;66:34–47.

53. Tawab AE, Abd AA, El Aal AS, mazied ME, Morsy EL. Prevalence of E. coli in broiler chickens in winter and summer seasons by application of PCR with its antibiogram pattern. Benha Vet Med J. 2015;29(2):119–28.
54. Bushen A, Tekalign E, Abayneh M. Drug and Multidrug-Resistance Pattern of *Enterobacteriaceae* isolated from droppings of healthy chickens on a Poultry Farm in Southwest Ethiopia. Infect Drug Resist. 2021;14:2051–8.
55. Younis G, Awad A, Mohamed N. Phenotypic and genotypic characterization of antimicrobial susceptibility of avian pathogenic Escherichia coli isolated from broiler chickens. Vet World. 2017;10:1167–72.
56. Amer MM, Bastamy MA, Ibrahim HM, Mervit MS. Isolation and characterization of avian pathogenic Escherichia coli from broiler chickens in some governorates of Egypt. VMJG. 2015;61:1–6.
57. Ibrahim AR, Cryer LT, Lafi QS, Abu-Basha E, Good L, Tarazi HY. Identification of Escherichia coli from broiler chickens in Jordan, their antimicrobial resistance, gene characterization and the associated risk factors. BMC Vet Res. 2019;15:159.
58. Sarowska J, Bozena FK, Agnieszka JK, Magdalena FM, Marta K, Gabriela BP, Irena CK. Virulence factors, prevalence and potential transmission of extraintestinal pathogenic *Escherichia coli* isolated from different sources: recent reports. Gut Pathol. 2019;11:10.
59. Maciel JF, Matter LB, Trindade MM, Camillo G, de LovatoM S, Castagna de Vargas A. Virulence factors and antimicrobial susceptibility profile of extraintestinal Escherichia coli isolated from an avian colisepticemia outbreak. Microb Pathog. 2017;103:119–22.
60. Obata-Yasuoka M, Ba-Thein W, Tsukamoto T, Yoshikawa H, Hayashi H. Vaginal Escherichia coli share common virulence factor profiles, serotypes and phylogeny with other extraintestinal *E. coli*. Microbiology. 2002;148:2745–52.
61. Germon P, Chen YH, He L, Jesu´s E, Blanco JS, Bre´e A, Schouler C, Huang SH, Moulin-Schouleur M. ibeA, a virulence factor of avian pathogenic Escherichia coli. Microbiology. 2005;151:1179–86.
62. Sedeek DM, Rady MM, Fedawy HS, Rabie NS. Molecular epidemiology and sequencing of avian pathogenic Escherichia coli APEC in Egypt. Adv Anim Vet Sci. 2020;8:499.
63. Knöbl T, Moreno MA, Paixão R, Tardelli Gomes AT,MônicaAparecidaMidolli, Vieira AM, Leite SD, Blanco EJ, Ferreira PA. Prevalence of avian pathogenic *Escherichia coli* (APEC) clone harboring *sfa* gene in Brazil. Sci World J.2012.
64. Johnson TJ, Wannemuehler Y, Doetkott C, JohnsonSJ, Rosenberger SC, Nolan LK. Identification of minimal predictors of avian pathogenic *Escherichia coli* virulence for use as a rapid diagnostic tool. J Clin Microbiol. 2008;46:3987–96.
65. Helal WMEA. Comparison between pathogenicity of E.coli serotypes isolated from intestinal and respiratory infections in chickens. M.V.Sc., Thesis, Fac. Vet. Med., Zagazig Univ, Egypt. 2012.
66. Wilczynski J, Stepien-Pysniak D, Wystalska D, Wernicki A. Molecular and serological characteristics of avian pathogenic Escherichia coli isolated from various clinical cases of Poultry Colibacillosis in Poland. Animals. 2022;12:1090.
67. De Carli S, Ikuta N, Lehmann FK, Da Silveira VP, DeMeloPredebon G, Fonseca AS, Lunge VR. Virulence gene content in *Escherichia coli* isolates from poultry flocks with clinical signs of colibacillosis in Brazil. PoultSci. 2015;94:2635–40.
68. Mohamed MA, Shehata MA, Rafeek E. Virulence genes content and Antimicrobial Resistance in *Escherichia coli* from broiler chickens. Vet Med Int. 2014.
69. Abd El-Tawab AA, El-Hofy FI, Alekhnawy kI, Talaie AT, Ahmed A. Insights into virulence and antimicrobial resistance plasmid associated genes of ESBL *Escherichia coli* associated with arthritis in chickens in Egypt. Int j adv res. 2018;7:174–82.
70. Ananias M, Yano T. Serogroups and virulence genotypes of Escherichia coli isolated from patients with sepsis. Braz J Med Biol Res. 2008;41:877–83.
71. Farooq S, Hussain I, MirMA, Bhat MA, Wani SA. Isolation of atypical enteropathogenic *Escherichia coli* and Shiga toxin 1 and 2f-producing *Escherichia coli* from avian species in India. Lett Appl Microbiol. 2009;48:692–7.
72. Zende RJ, Chavhan DM, Suryawanshi PR, Rai AK, Vaidya VM. PCR detection and serotyping of enterotoxigenic and shigatoxigenic *Escherichia coli* isolates obtained from chicken meat in Mumbai, India. Vet World. 2013;6:770–3.
73. Samanta I, Joardar SN, Das PK, Sar TK. Comparative possession of Shiga toxin, intimin, enterohaemolysin and major extended spectrum beta lactamase (ESBL) genes in *Escherichia coli* isolated from backyard and farmed poultry. Iran J Vet Res. 2015;16:90–3.
74. Manges AR, Perdreau-Remington F, Solberg O, Riley LW. Multi drug resistant Escherichia coli clonal groups causing community-acquired bloodstream infections. J Infect. 2006;53:25–9.
75. Jakobsen L, Garneau P, Bruant G, Harel J, Olsen SS, Porsbo LJ, Frimodt-Møller N. Is Escherichia coli urinary tract infection a zoonosis? Proof of direct link with production animals and meat. Eur J Clin MicrobiolInfect Dis. 2012;31:1121–9.
76. Ghorbani HR, Mehr FP, Pazoki H, Rahmani BM. Synthesis of ZnO nanoparticles by precipitation method. Orient J Chem.2015:1219–21.
77. TiwariM, Jain P, Hariharapura RC, NarayananK, Bhat U, Udupa N, Rao JV. Biosynthesis of copper nanoparticles using copper-resistant Bacillus cereus, a soil isolate. Process Biochem. 2016;51:1348–56.
78. Rajendaran K, Muthuramalingam R, Ayyadurai S. Green synthesis of Ag-Mo/CuO nanoparticles using Azadirachta indica leaf extracts to study its solar photocatalytic and antimicrobial activities. Mater Sci Semicond Process MAT SCI SEMICON PROC. 2019; 91: 230–238.
79. SebeiaN, Jabli M, Ghith A. Biological synthesis of copper nanoparticles, using Nerium oleander leaves extract: characterization and study of their interaction with organic dyes. Inorg Chem Commun. 2019;105:36–46.
80. El-Batal AI, Mosalam FM, Ghorab MM, Hanora A, Elbarbary AM. Antimicrobial, antioxidant and anticancer activities of zinc nanoparticles prepared by natural polysaccharides and gamma radiation. Int J Biol Macromol. 2018;107:2298–311.
81. De Barros HR, Cardoso MB, de Oliveira CC, Franco CRC, de Lima Belan D, VidottiM, Riegel-Vidotti IC. Stability of gum arabic-gold nanoparticles in physiological simulated pHs and their selective effect on cell lines. RSC Adv. 2016;6:9411–20.
82. Rabeea MA, DaoubAarif Elmubarak H, Misni Misran Elfatih A, Hassan Mohammed Osman E. Characterization and functional properties of some natural Acacia gums. J Saudi SocAgricSci. 2016;17:241–9.
83. Ba-Abbad MM, TakriffMS, BenamorA, Mahmoudi E, Mohammad AW. Arabic gum as green agent for ZnO nanoparticles synthesis: properties, mechanism and antibacterial activity. J Mater Sci : Mater Electron. 2017;28:12100–7.
84. OtteHM. Lattice parameter determinations with an X-ray spectrogoniometer by the Debye-Scherrer method and the effect of specimen condition locality: synthetic. J Appl Phys. 1961;32:1536–46.
85. Baneeva MI, Popova SV. The analysis of zinc hydroxide under high pressures and temperatures. Geokhimiya. 1969:1014–6.
86. Naz S, Gul A, Zia M. Toxicity of copper oxide nanoparticles: a review study. IET Nanobiotechnol. 2020;14:1–13.
87. Lok CN, HoCM ChenR, He QY, Yu WY, Sun H, TamPK, Chiu JF, Che CM. Proteomic analysis of the mode of antibacterial action of silver nanoparticles. J Proteome Res. 2006;5:916–24.
88. Kim JS, Kuk E, Yu KN, Kim JH, Park SJ, Lee HJ, Kim SH, Park YK, Park YH, HwangCY, Kim YK, Leem YS, Jeong DH. ChoMH. Antimicrobial effects of silver nanoparticles. Nanomedicine. 2007;3:95–101.
89. McQuillanJ. Bacterial-Nanoparticle Interactions. Thesis for the degree of Doctor of Philosophy in Biological Sciences. University of Exeter. 2010.
90. Pandurangan M, Kim DH. In vitro toxicity of zinc oxide nanoparticles: a review. J Nanoparticle Res. 2015;17:1–8.
91. Shi M, Kwon HS, Peng Z, ElderA YangH. Effects of surface chemistry on the generation of reactive oxygen species by copper nanoparticles. ACS Nano. 2012;6:2157–64.
92. Prasad PR, Kanchi S, Naidoo EB. In-vitro evaluation of copper nanoparticles cytotoxicity on prostate cancer cell lines and their antioxidant, sensing and catalytic activity: one-pot green approach. J Photochem Photobiol B Biol J. 2016;161:375–82.
93. Ramchandani M, Manges AR, DebRoy C, Smith SP, Johnson JR, Riley LW. Possible animal origin of Human-Associated, Multidrug-Resistant, Uropathogenic Escherichia coli. Clin Infect Dis. 2005;40:251–7.
94. Massot M, Daubié AS, Clermont O, Jaureguy F, Couffignal C, Dahbi G, Denamur E. Phylogenetic, virulence and antibiotic resistance characteristics of commensal strain populations of Escherichia coli from community subjects in the Paris area in 2010 and evolution over 30 years. Microbiology. 2016;162:642.
95. Abdollahi Z, Zare EN, Salimi F, Goudarzi I, Tay FR, Makvandi P. Bioactive carboxymethyl starch-based hydrogels decorated with CuO nanoparticles: antioxidant and Antimicrobial Properties and Accelerated Wound Healing in vivo. Int J MolSci. 2021;22:2531.
96. Dehghani S, Peighambardoust SH, Peighambardoust SJ, Fasihnia SH, Khosrowshahi NK, Gullón B, Lorenzo JM. Optimization of the amount of ZnO, CuO, and Ag Nanoparticles on Antibacterial Properties of low-density polyethylene (LDPE) Films using the response surface method. Food AnalMethods. 2021;14:98–107.
97. Rajeshkumar S, Menon SI, Kumar SV, Ponnanikajamideen M, Ali D, Arunachalam K. Anti-inflammatory and antimicrobial potential of Cissus quadrangularis-assisted copper oxide nanoparticles. J Nanomater. 2021.

98. Chakraborty R, Sarkar RK, Chatterjee AK, Manju U, Chattopadhyay AP, Basu T. A simple, fast and cost-effective method of synthesis of cupric oxide nanoparticle with promising antibacterial potency: unraveling the biological and chemical modes of action. Biochim Biophys Acta Gen Subj. 2015;1850:845–56.
99. Su Y, Zheng X, Chen Y, Li M, Liu K. Alteration of intracellular protein expressions as a key mechanism of the deterioration of bacterial denitrification caused by copper oxide nanoparticles. Sci. 2015;5:15824.
100. Radi AM, Abdel Azeem NM, EL-Nahass ELS. Comparative effects of zinc oxide and zinc oxide nanoparticle as feed additives on growth, feed choice test, tissue residues, and histopathological changes in broiler chickens. Environ Sci Pollut Res. 2021;28:5158–67.
101. Ruiz P, Katsumiti A, Nieto JA, Bori J, Jimeno-Romero A, Reip P, Arostegui I, Orbea A, Cajaraville MP. Short-term effects on antioxidant enzymes and long-term genotoxic and carcinogenic potential of CuO nanoparticles compared to bulk CuO and ionic copper in mussels Mytilusgalloprovincialis. Mar Environ Res. 2015;111:107–20.
102. Azam A, Ahmed AS, Oves M, Khan MS, Habib SS, Memic A. Antimicrobial activity of metal oxide nanoparticles against gram-positive and gram-negative bacteria: a comparative study. Int J Nanomedicine. 2012;7:6003–9.
103. Sizova E, MiroshnikovS, Balakirev N. Forecast of productive and biological effects of metal nanoparticles according to tolerance index. Int J GEOMATE. 2019;17:141–8.
104. Díaz-Visurraga J, Gutiérrez C, Von Plessing C, García A. Metal nanostructures as antibacterial agents. Sci against Microb pathogens: commun curr res technol adv. 2011;1:210–8.
105. Agarwala M, Choudhury B, Yadav RNS. Comparative study of antibiofilm activity of copper oxide and iron oxide nanoparticles against multidrug resistant biofilm forming uropathogens. Indian JMicrobiol. 2014;54:365–8.
106. Morsy EA, Hussien AM, Ibrahi MA, Farroh KY, Hassanen El. Cytotoxicity and genotoxicity of copper oxide nanoparticles in chickens. Biol Trace Elem Res. 2021;199:4731–45.
107. Du BD, Phu DV, QuocLA, Hien NQ. Synthesis and investigation of antimicrobial activity of Cu2O Nanoparticles/Zeolite. J Nanopart. 2017: 1–6.
108. Fariba A, Bahram EG, Farrokh K, Tabrizy S, Pooneh SS. An investigation of the effect of copper oxide and silver nanoparticles on *E. Coli* Genome by Rapd Molecular markers. J Adv Biotechnol Microbiol. 2016;1:1–6.
109. Awaad MHH, El. Moustafa KM, Zoulfakar SA, Elhalawany MS, MohammedFF, El-RefayRM, Morsy EA. The role of silver nanoparticles in the reluctance of colisepticemia in broiler chickens. J Appl Poult Res. 2021;30:100155.
110. Rosa G, Alba DF, Silva AD, Gris A, Mendes RE, Mostardeiro VB. Impact of *Escherichia coli* infection in broiler breeder chicks: the effect of oxidative stress on weight gain. Microb Pathog. 2020;139:103861.
111. El-kazaz SE, Hafez MH. Evaluation of copper nanoparticles and copper sulfate effect on immune status, behavior, and productive performance of broilers. J Adv Vet Anim Res. 2019;7:16–25.
112. Sarvestany SS, Resvani M, Zamiri M, ShekarforoushS, Atashi H, MoslehN. The effect of nanocopper and mannan oligosaccharide supplementation on nutrient digestibility and performance in broiler chickens. J Vet Res. 2016;71:153–61.
113. Scott A, Vadalasetty KB, Chwalibog A, Sawosz E. Copper nanoparticles as an alternative feed additive in poultry diet: a review. Nanotechnol Rev. 2018;7:69–93.
114. Mavrommatis A, Giamouri E, Tavrizelou S, Zacharioudaki M, Danezis G, Simitzis PE, Feggeros K. Impact of mycotoxins on animals' oxidative status. Antioxidants. 2021;10:214.
115. Balakrishna S, Prabhune AA. Gamma-glutamyl transferases: a structural, mechanistic and physiological perspective. FrontBiol. 2014;9:51–65.
116. Manafi M, Khalaji S, Hedayati M, Pirany N. Efficacy of *Bacillus subtilis* and bacitracin methylene disalicylate on growth performance, digestibility, blood metabolites, immunity, and intestinal microbiota after intramuscular inoculation with *Escherichia coli* in broilers. Poult Sci. 2017;96:1174–83.
117. El-Kassas S, El-Nagggar K, Abdo SE, Abdo W. AbeerAK. Dietary supplementation with coper oxide nanoparticles ameliorates chronic heat stress in broiler chickensAnim. Prod Sci. 2020;60:254–68.
118. Lee IC, Kim JC, Ko JW, Park SH, Lim JO, Shin IS, Moon C, Kim SH, Her JD. Comparative toxicity and biodistribution of copper nanoparticles and cupric ions in rats. Int J Nanomedicine. 2016;11:2883–900.
119. AbdelazeimSA, Shehata NI, Aly HF, Shams SG. Amelioration of oxidative stress–mediated apoptosis in copper oxide nanoparticles–induced liver injury in rats by potent antioxidants. Sci. 2020;10:1–14.
120. Elkhateeb SA, Ibrahim TR, El-Shal AS, Abdel Hamid OI. Ameliorative role of curcumin on copper oxide nanoparticles mediated renal toxicity in rats: an investigation of molecular mechanisms. J Biochem Mol Toxicol. 2020;34:e22593.
121. Cholewińska E, Ognik K, Fotschki B, Zduńczyk Z, Juśkiewicz J. Comparison of the effect of dietary copper nanoparticles and one copper (II) salt on the copper biodistribution and gastrointestinal and hepatic morphology and function in a rat model. PLoS ONE. 2018;13:e0197083.
122. Ghasemipoor M, Zolghadri S. The effect of copper oxide nanoparticles as feed additive on some the blood proteins of broiler chickens. Mol Biol Commun. 2014;3:144.
123. Scott A, Vadalasetty KP, Lukasiewicz M, Jaworski S, Wierzbicki M, Chwalibog A, Sawosz E. Effect of different levels of copper nanoparticles and copper sulphate on performance, metabolism and blood biochemical profiles in broiler chicken. J Anim Physiol Anim Nutr. 2017;102:364–73.
124. Boya P, Reggiori F, Codogno P. Emerging regulation and functions of autophagy. Nat Cell Biol. 2013;15:713–20.
125. Arancibia S, Barrientos A, Torrejón J, Escobar A, Beltrán CJ. Copper oxide nanoparticles recruit macrophages and modulate nitric oxide, pro inflammatory cytokines and PGE2 production through arginase activation. Nanomedicine. 2016;11:1237–51.
126. Elsabahy M, Wooley KL. Cytokines as biomarkers of nanoparticle immunotoxicity. Chem Soc Rev. 2013;42:5552–76.
127. Niehues T. C-reactive protein and other biomarkers- the sense and non-sense of using inflammation biomarkers for the diagnosis of severe bacterial infection. Lympho Sign J. 2018;5:35–47.
128. Dai W, Qi C, WangS. Synergistic effect of glucosamine and vitamin E against experimental rheumatoid arthritis in neonatal rats. BiomedPharmacother. 2018;105:835–40.
129. Faisal S, Jan H, Alam I, Rizwan M, Hussain Z, Sultana K, Ali Z, Uddin MZ. In Vivo Analgesic, Anti-Inflammatory, and Anti-Diabetic Screening of Bacopa monnieri-Synthesized Copper Oxide Nanoparticles. ACS Omega, 2022; 7: 4071 – 4082.
130. Martinez-de-Anda A, Valdivia AG, Jaramillo-Juarez F, Reyes JL, Ortiz R, Quezada T, Rodríguez ML. Effects of aflatoxin chronic intoxication in renal function of laying hens. Poult Sci. 2010;89:1622–8.
131. AbbasS JM, Ahmad Khan H, Rahman K. Toxicity and bioaccumulation of metals (Al and Co) in three economically important carnivorous fish species of PakistanInt. J Agric Biol. 2018;20:1123–8.
132. Tunçsoy M, Duran S, Ay Ö, Cicik B, ErdemC. Effects of copper oxide nanoparticles on antioxidant enzyme activities and on tissue accumulation of Oreochromis niloticus. Bull Environ Contam Tox. 2017;99:360–4.
133. Sawosz E, Łukasiewicz M, Łozicki A, Sosnowska M, Jaworski S, Niemiec J, Chwalibog A. Effect of copper nanoparticles on the mineral content of tissues and droppings, and growth of chickens. Arch Anim Nutr. 2018;72:396–406.
134. Ognik K, Stepniowska A, Cholewi´nska E, Kozlowski K. The effect of administration of copper nanoparticles to chickens in drinking water on estimated intestinal absorption of iron, zinc, and calcium. Poult Sci. 2016;95:2045–51.
135. Ognik K, Cholewińska E, Stępniowska A, Drażbo A, Kozłowski K, Jankowski J. The effect of administration of copper nanoparticles in drinking water on redox reactions in the liver and breast muscle of broiler chickens. Ann Anim Sci. 2019;19:663–77.
136. SizovaE, Miroshnikov S, Lebedev S, Usha B, Shabunin S. Use of nanoscale metals in poultry diet as a mineral feed additive. Anim Nutr. 2020;6:185–91.

Publisher's Note